NEXT Performance Curve Analysis And Validation

Pratik Saripalli*
Graduate Research Assistant, College Park, Maryland, 20740, USA
Eric Cardiff† and Jacob Englander ‡
NASA Goddard Space Flight Center, Greenbelt, Maryland, 20770, USA

Performance curves of the NEXT thruster are highly important in determining the thruster's ability in performing towards mission-specific goals. New performance curves are proposed and examined here. The Evolutionary Mission Trajectory Generator (EMTG) is used to verify variations in mission solutions based on both available thruster curves and the new curves generated. Furthermore, variations in BOL and EOL curves are also examined. Mission design results shown here validate the use of EMTG and the new performance curves.

Nomenclature

$\dot{m}$	Mass flow rate, mg/s
T	Thrust, N
Isp	Specific impulse, sec
V_{bps}	Beam power supply voltage, V
BOL	Beginning of life
EOL	End of life
P_{in}	Input Power, kW

I. Introduction

Electric propulsion (EP) systems are required to perform within a wide range of requirements depending on the mission. In order to accomplish this, proper performance characterization is required to understand each thruster's capabilities and limits for mission design analysis and evaluation.

NASA's Evolutionary Xenon Thruster (NEXT) is a flight-qualified gridded electrostatic system that is capable of offering two and a half times the thrust of the of the NSTAR ion engines.[1] In order for it to be considered for future missions, its capabilities as an EP thruster must be quantified for mission planning, calling for a set of throttle curves that can characterize the thruster's operating limits. These curves plot the thrust (T) and mass flow rate ($\dot{m}$) as a function of input power at constant beam power supply voltage (V_{bsp}). The V_{bsp} ranges from 275 V (low power) to 1800 V. The throttle table is shown in Table 1, below. Each V_{bsp} at a certain input power level is defined as a"throttle point". Forty throttle points have been identified for NEXT, with each combination representing a unique beam voltage and current.[2,3] NEXT has been designed to operate between 0.6 - 7.2 kW input power. The throttle curves described in this paper aim to represent the performance capabilities of NEXT.

*Graduate Research Assistant, Department of Aerospace Engineering, University of Maryland, College Park, 20740
†Senior Propulsion Engineer, Propulsion Branch (CODE 597), NASA Goddard Space Flight Center
‡Systems Engineer, Mission Design Branch (CODE 595), NASA Goddard Space Flight Center

Beam Current, A	Beam Power Supply Voltage (Vbps), V												
	1800	1567	1396	1179	1021	936	850	700	679	650	400	300	275
3.52	TL40	TL39	TL38	TL37	ETL3.52A	ETL3.52B	ETL3.52C	ETL3.52D					
3.10	TL36	TL35	TL34	TL33	ETL3.1A	ETL3.1B	ETL3.1C	ETL3.1D	ETL3.1E				
2.70	TL32	TL31	TL30	TL29	TL28	ETL2.7A	ETL2.7B	ETL2.7C	ETL2.7D	ETL2.7E			
2.35	TL27	TL26	TL25	TL24	TL23	ETL2.35A	ETL2.35B	ETL2.35C	ETL2.35D	ETL2.35E			
2.00	TL22	TL21	TL20	TL19	TL18	ETL2.0A	ETL2.0B	ETL2.0C	ETL2.0D	ETL2.0E			
1.60	TL17	TL16	TL15	TL14	TL13	ETL1.6A	ETL1.6B	ETL1.6C	ETL1.6D	ETL1.6E	ETL1.6F		
1.20	TL12	TL11	TL10	TL09	TL08	TL07	TL06		TL05	TL04	TL03	TL02	
1.00													TL01

Table 1: Input parameters for the throttle points available for the NEXT thruster.

NASA Glenn Research Center (GRC) has released high thrust and high Isp throttle curves that have been used in mission designs for the Discovery and New Frontiers proposal calls. However, this paper suggests that these curves might not be adequate to accurately quantify the thruster's performance. Trajectory optimizers use throttle curves to find the best solutions for a required mission objective. By not having numerous or accurate curves that can fully characterize a thruster, mission solutions won't be fully optimized. Mission trajectories will vary depending on the thruster curve used, resulting in an inability to reproduce an optimized solution. Furthermore, if degradation of thruster performance due to regular operation isn't accounted for, more inaccuracies can occur. Therefore, validation of thruster curves is necessary for proper thruster performance characterization. A global trajectory optimizer (such as EMTG, discussed later) is required to test each throttle curve against specific mission requirements.

II. Engine Models

A. New Throttle Curves

Each throttle point shown in Table 1 has documented beginning of life (BOL) and end of life (EOL) data describing $\dot{m}$ and T. Using these values, separate thruster curves were generated for each V_{bsp} at both BOL and EOL. In order to have a continuous curve, a 4th-order polynomial best fit was applied to each curve. These curves can be found in the Appendix. None of the fit lines have a R^2 value lower than 0.99, verifying good representation of the data. Furthermore, BOL and EOL high thrust and high Isp curves were also generated using the highest thrust and $\dot{m}$ values at each V_{bsp}. Throughout the paper, the 1800 V_{bsp} BOL and EOL curves along with the BOL and EOL high thrust curves were used to compare with the GRC curves. Data was taken from Throttle Table 11, released by GRC.[4]

Figures 1 and 2 show the thruster curves for thrust and $\dot{m}$ at each V_{bsp}, BOL and EOL. Each plot includes the discrete data points as well as the fit lines. Note that the lowest V_{bsp} fit line shown is 400 V. The 275 V_{bsp} and 300 V_{bsp} fit lines are not shown for clarity purposes.

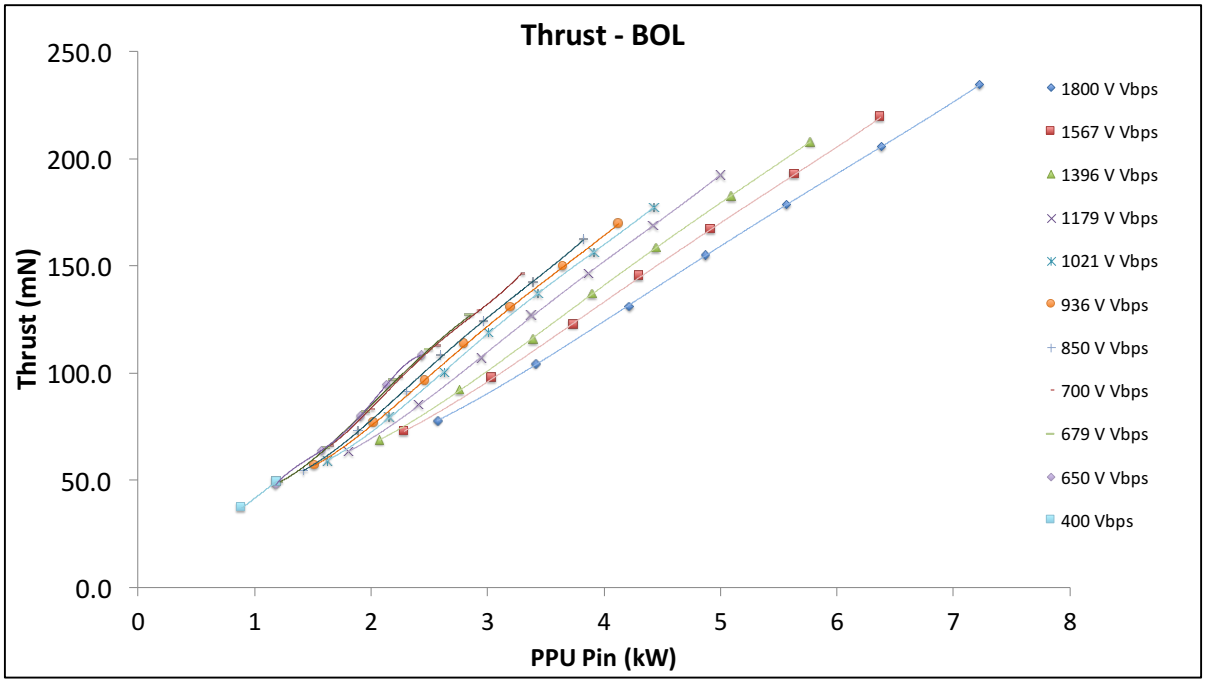

(a) Thrust curves

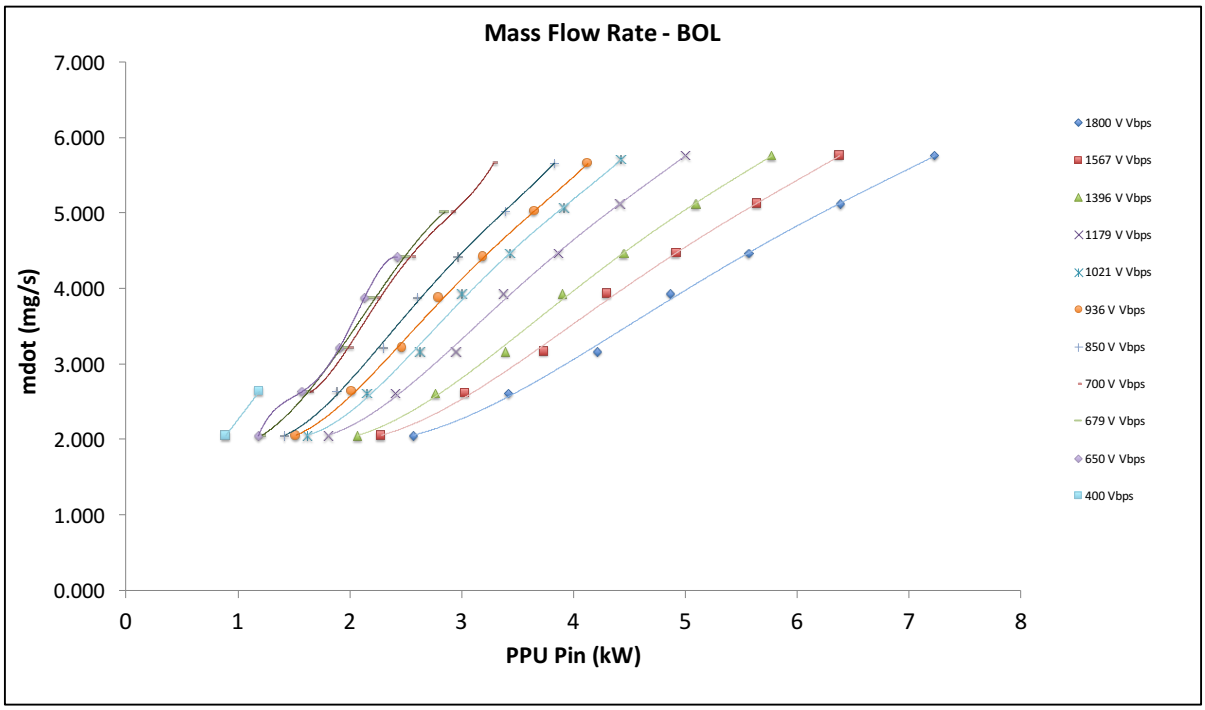

(b) Mass flow rate curves

Figure 1: Throttle curves at BOL

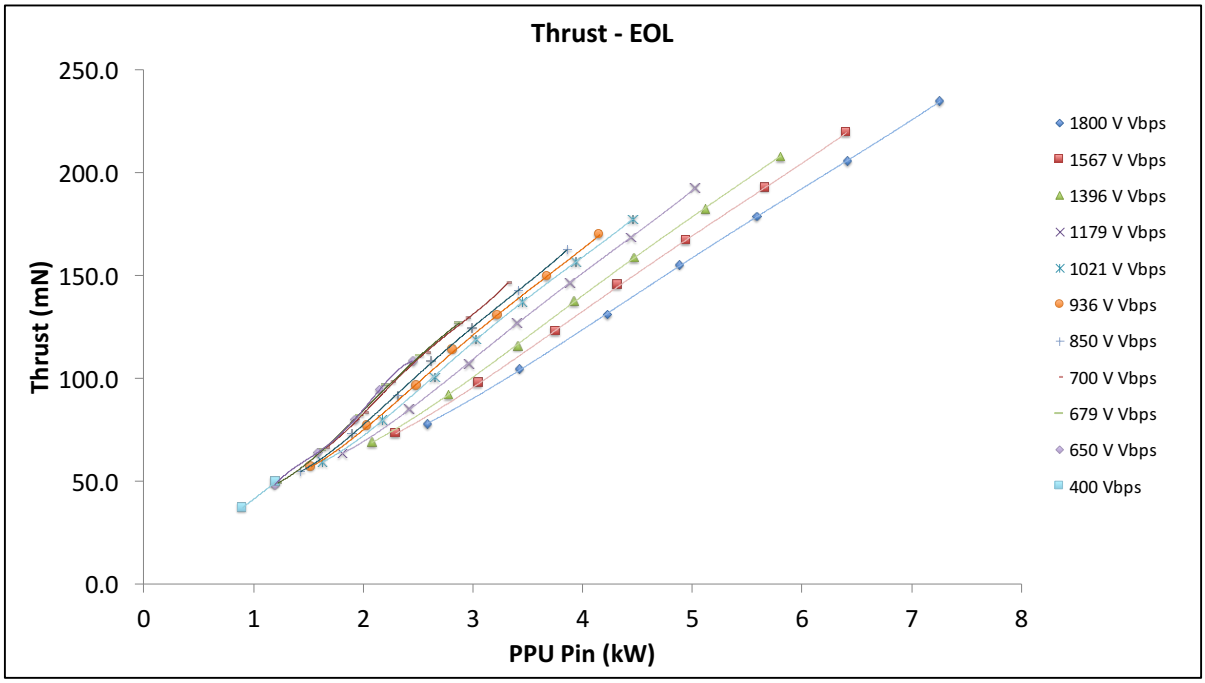

(a) Thrust curves

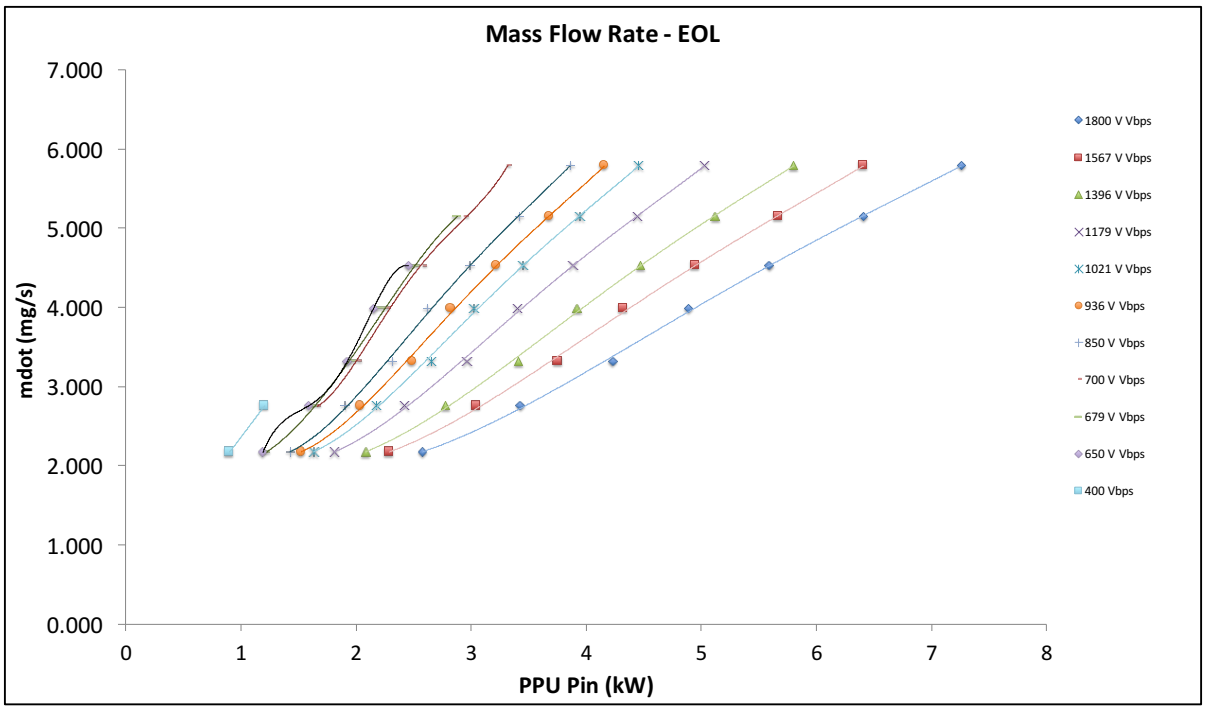

(b) Mass flow rate curves

Figure 2: Throttle curves at EOL

As can be seen in Figures 1 and 2, there are no data points to represent the low-power regime for the high voltage curves, especially for the 1800 V curve. This forces the polynomial fit to inaccurately represent the thrust and mass flow rate at low power. Therefore, data points from lower voltage curves were used to generate modified fit-lines at 1800 V. These are shown below (Figures 3 and 4). The points shown in red represent the original 1800 V data whereas the points shown in blue represent the modified 1800 V data. It is clear that the modified curves have better representation of the low-power regime. In addition to the modified 1800 V curves, high thrust and high Isp curves were also generated. Table 2 visualizes the throttle points used for the hight thrust and high Isp curves as well as the modified 1800 V curves. The green line in Figure 2a shows the throttle points used for the high thrust curves. The red line in Figure 2b shows the throttle points used for the high Isp curves. Figure 2b also shows the throttle points used for the modified 1800 V curves, marked by the dashed yellow line. Figure 5 plots these new throttle curves alongside others previously generated.

Before moving on, it is beneficial to address the validity of the approach used to generate the modified 1800 V curves. The modified 1800 V curves use similar throttle points to the high Isp curves (see Table 2b). The only difference is fewer points were used in defining the low power regime of the 1800 V curve. This was to ensure the modified 1800 V curve was still a predominantly 1800 V_{bsp} curve but still have some representation in the low power regime. Therefore, the modified 1800 V curve is a hybrid between the full 1800 V curve and a high Isp curve. Both of these curves, along with the curves mentioned above, were used in the mission analysis discussed latter in the paper.

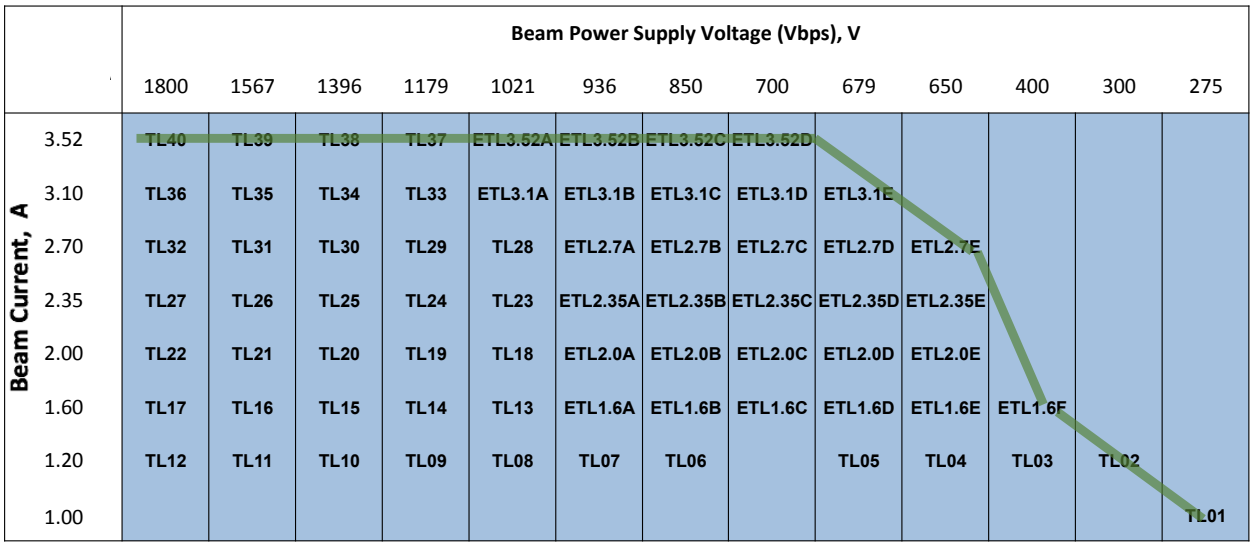

(a) High thrust curve throttle points

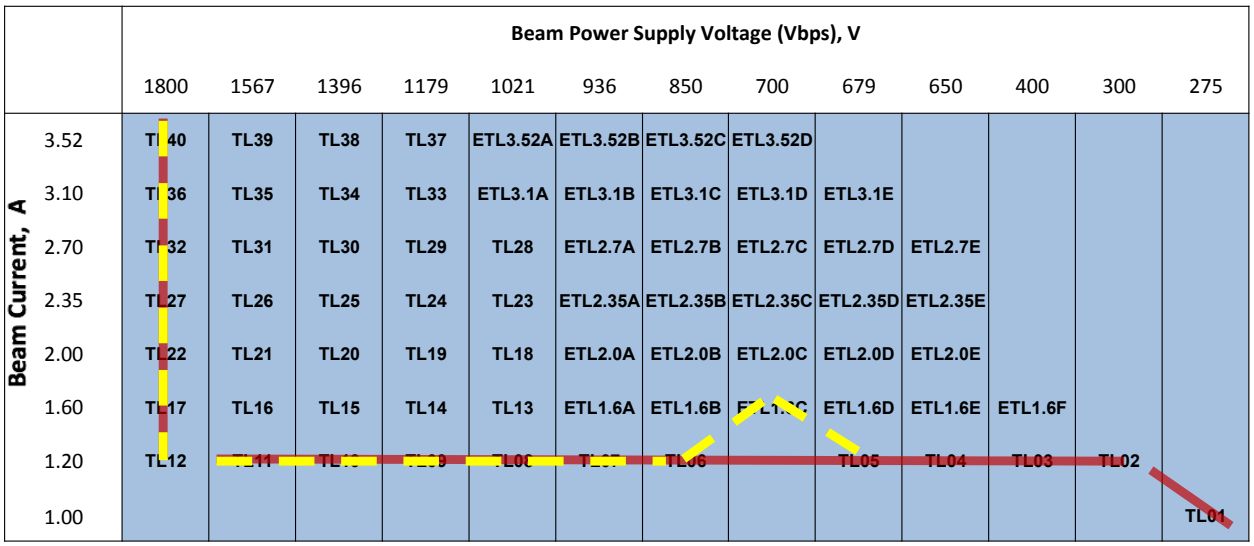

(b) High Isp (red) and 1800 V (dashed yellow) curve throttle points

Table 2: Throttle points used for the high thrust and high Isp curves

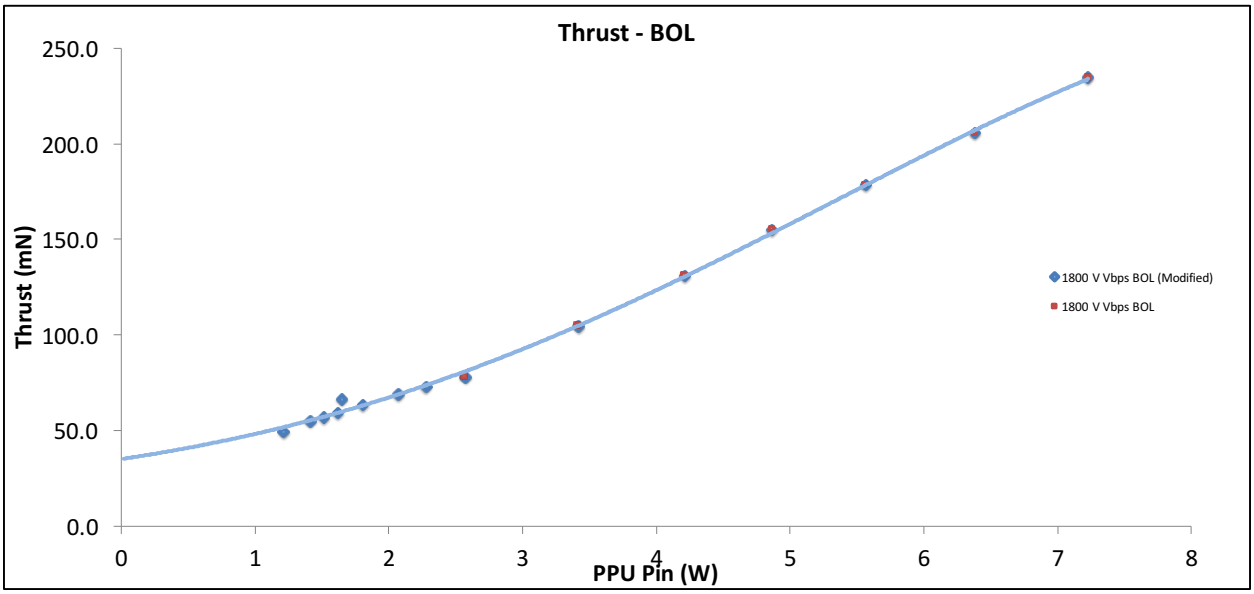

(a) Thrust curves

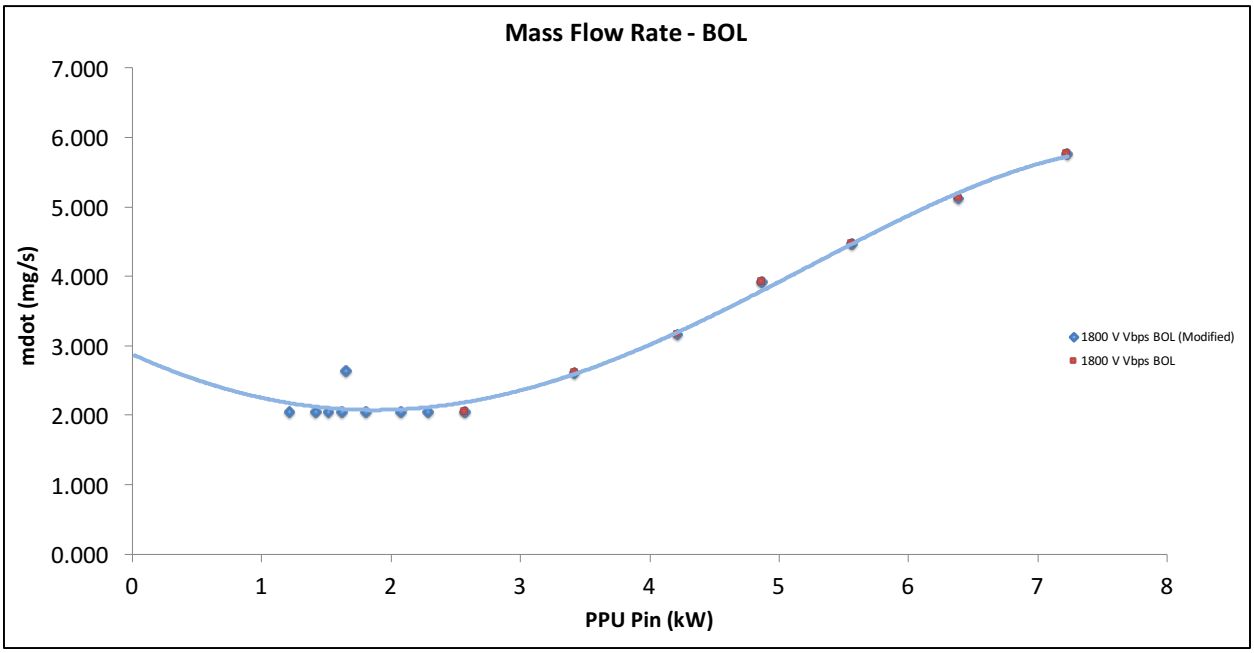

(b) Mass flow rate curves

Figure 3: Throttle curves for 1800 V at BOL

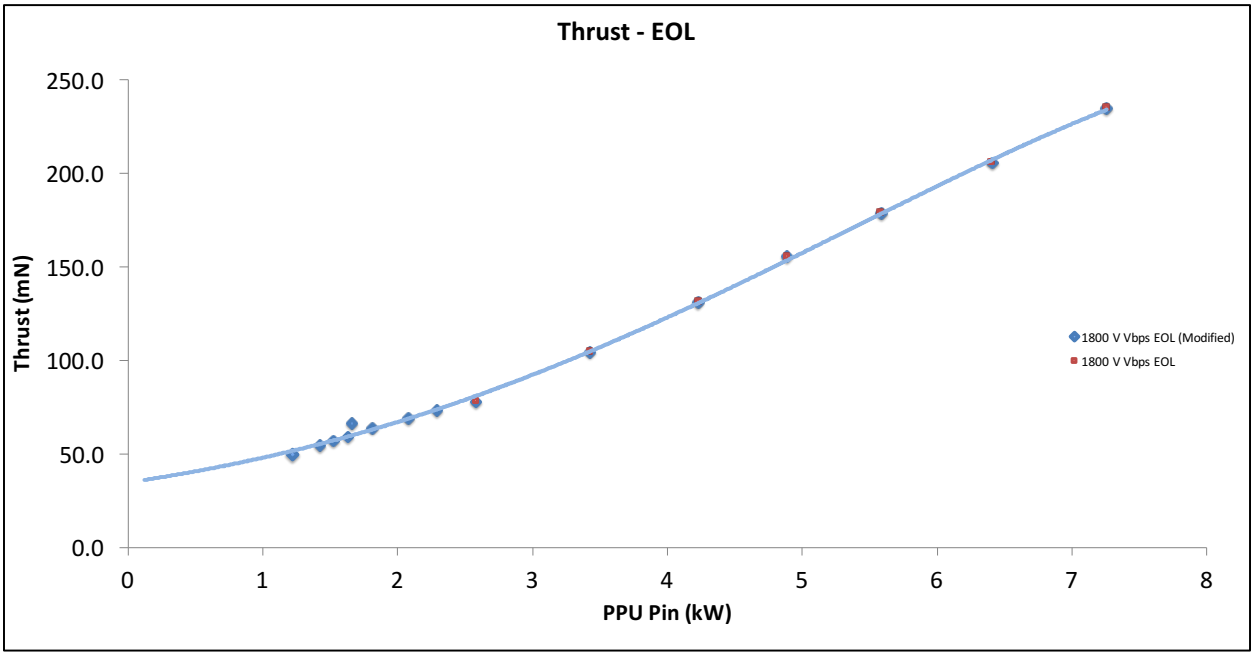

(a) Thrust curves

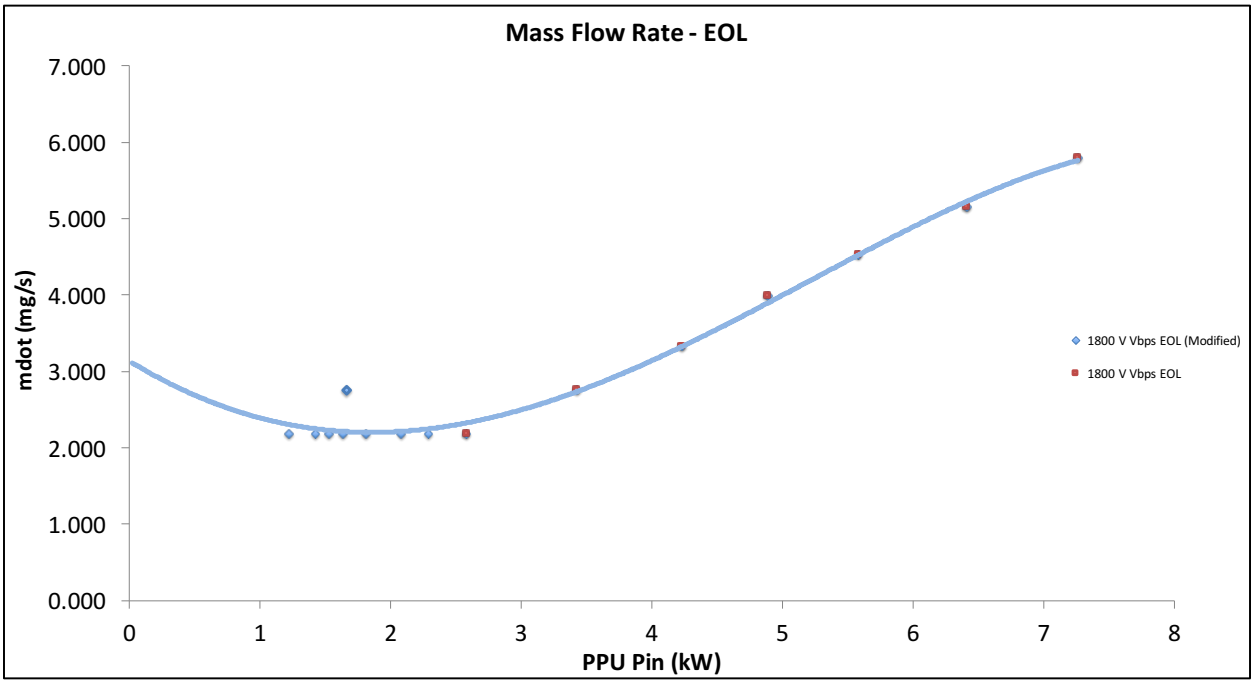

(b) Mass flow rate curves

Figure 4: Throttle curves for 1800 V at EOL

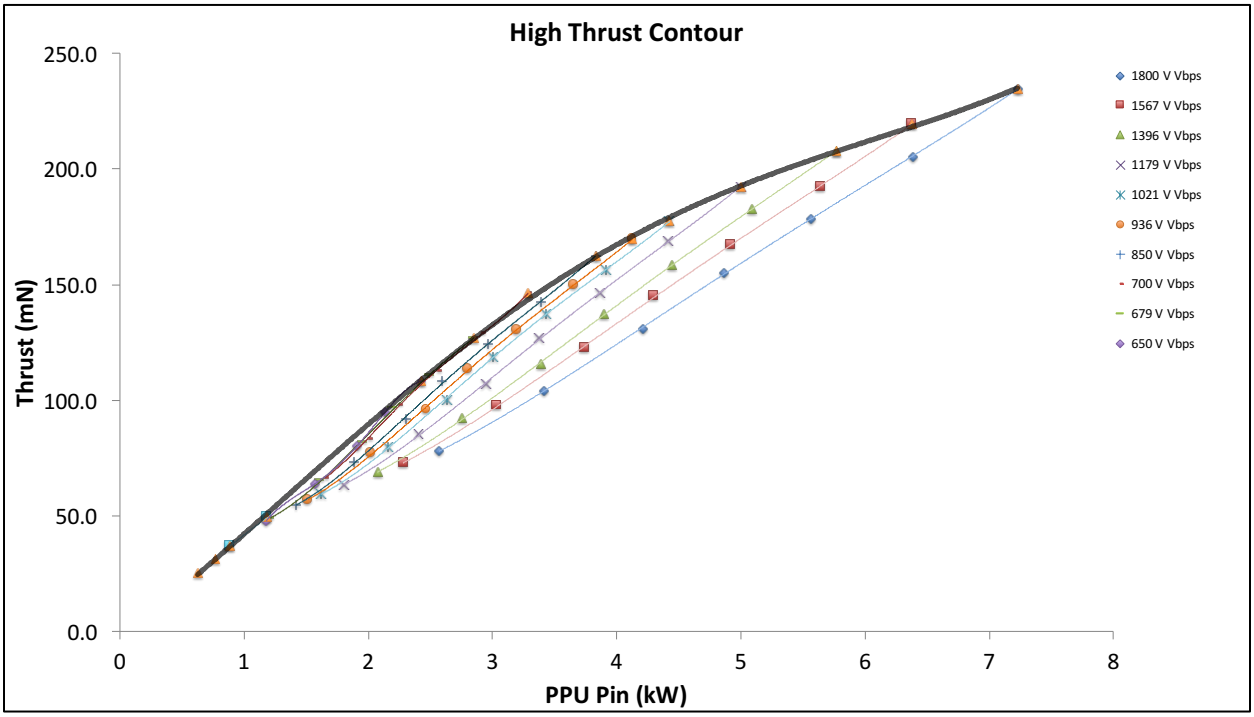

(a) High thrust contour polynomial

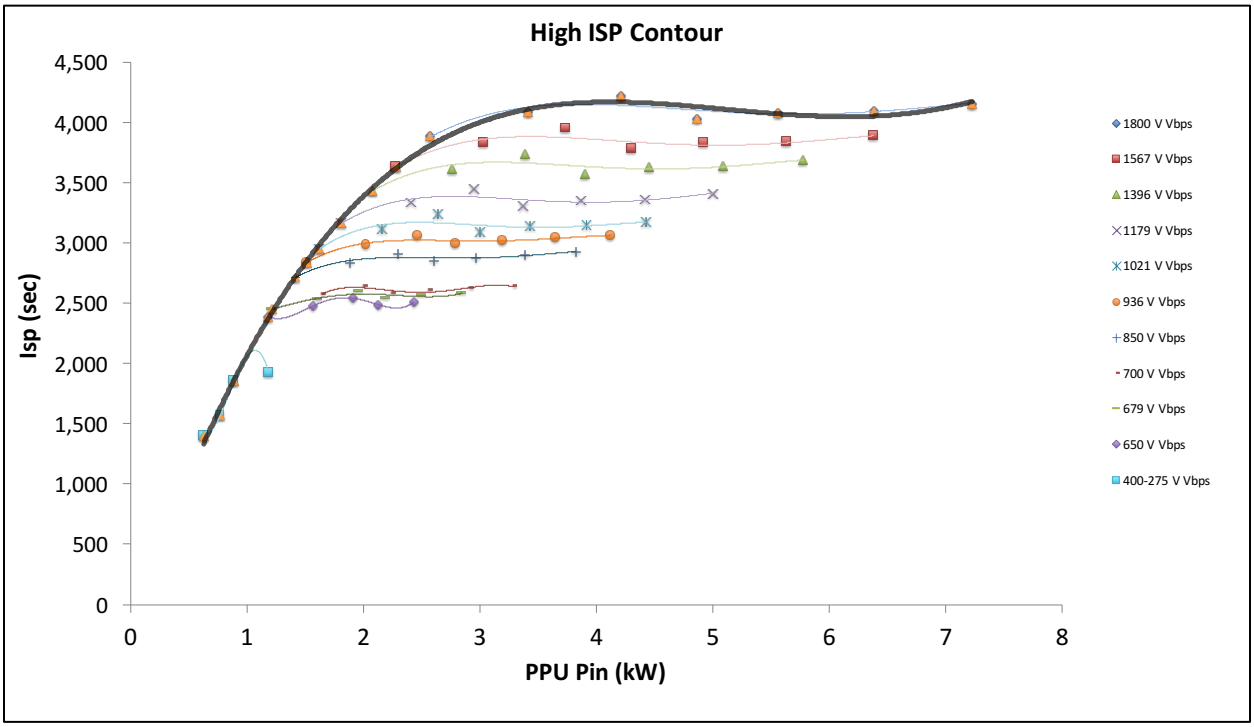

(b) High Isp contour polynomial

Figure 5: Contour plots for high thrust and high Isp

B. GRC Curves

NASA GRC has documented multiple curve fits that are currently being used for mission analysis. According to the 2014 NEXT Discovery AO,[4] the GRC high thrust curves are broken up into baseline throttle level and an extended throttle level (ETL) curves. An effort has been made to extract which throttle points were used to generate the GRC high thrust and high Isp curves (Tables 3a and 3b).

The equations for all the fit lines are shown in Tables 9, 10, 11, and 12 located in the appendix section. The high Isp and high thrust equations are also listed. Tables 13, 14, 15 and 16 show the equations for GRC high thrust and GRC high thrust ETL curves. The GRC high Isp equations are listed in Tables 17 and 18. Note that the independent variable for these equation is P_{in}.[a].

[a]Higher significant figures were used for the 1800 V_{bsp} to ensure no error at full power

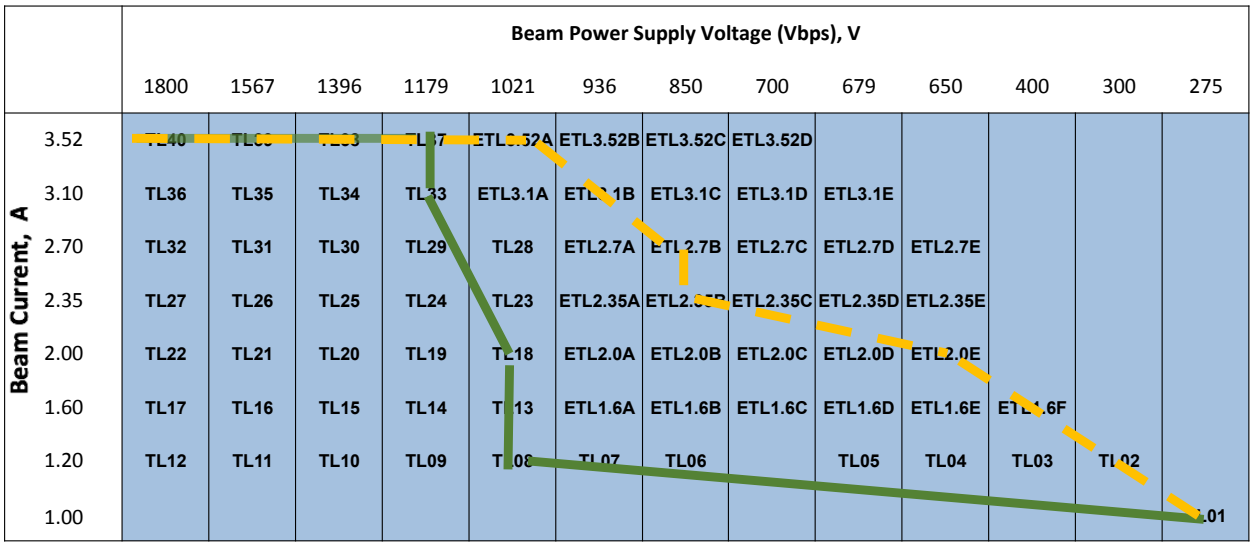

(a) GRC High Thrust (green) and GRC High Thrust ETL (dashed yellow) curve throttle points

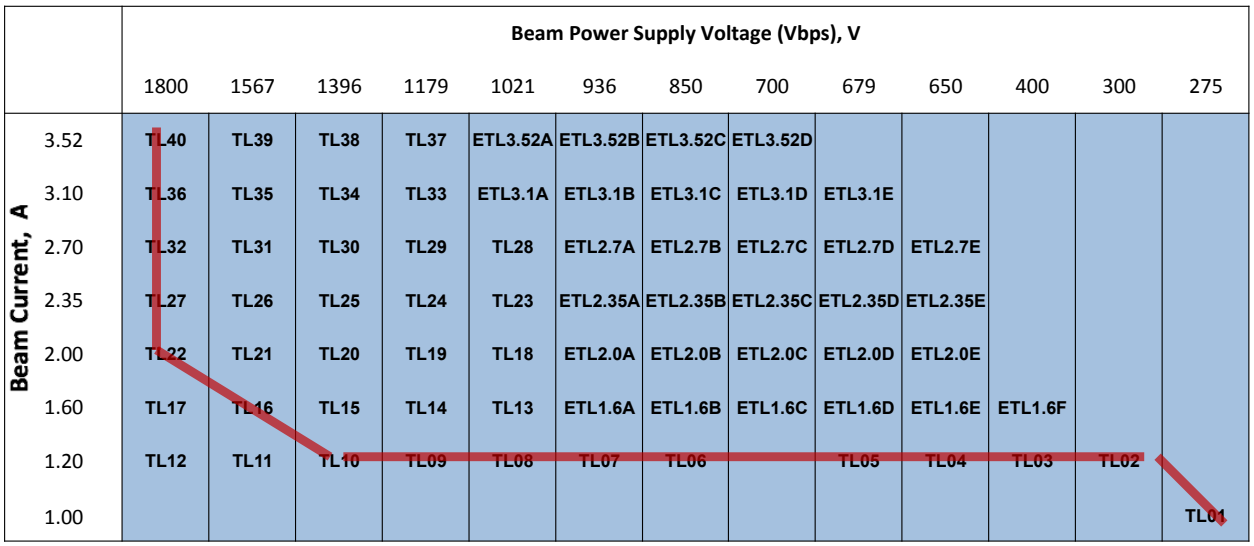

(b) GRC High Isp contour throttle points

Table 3: Potential throttle points used for GRC high thrust and high Isp curve

C. Comparision

The following figures compare the GRC high thrust and high Isp curves with the author's high thrust and high Isp curves (Figures 6 and 7). The black lines represent the high thrust and Isp curves generated by the authors in this paper and the blue represent the baseline GRC high thrust and high Isp curves for NEXT. Specific to the high thrust plots, the red lines represent the GRC high thrust ETL curves.

The GRC high Isp curves and the author's high Isp curves are relatively close to each other with some areas at which the thrust and mass flow rate curves vary slightly. It is expected that there will be small variations when using these curves for mission design, which will be addressed below. The high thrust curves, on the other hand, have a larger discrepancy between them. This paper's high thrust curves used throttle points that maximized thrust (maximizing beam current at lower levels of beam power supply voltage). The GRC and GRC ETL curves used throttle points with lower beam current levels at lower beam power supply voltage).

Figures 8 and 9, below, plot each of throttle curves on thrust vs input power and mass flow rate vs input power graphs. The curves are broken up into high thrust and high Isp categories. As is shown, there is some variation between curves, especially between the GRC curves and the curves generated in this paper. These variations do have an effect on mission planning as explored further in the paper.

In particular, in Figure 6 the high thrust curve produces the same amount of thrust as the GRC curves at both ends of input power (low and high power) but higher thrust at powers from 1 kW to 6 kW. In Figure 7, the 1800 V BOL/EOL curves are higher in thrust and lower in Isp than the GRC curves at low power but provide similar amounts of thrust at higher Isp's at powers 2 kW to 5 kW. Figures 8 and 9 plot all the curves used for mission analysis.

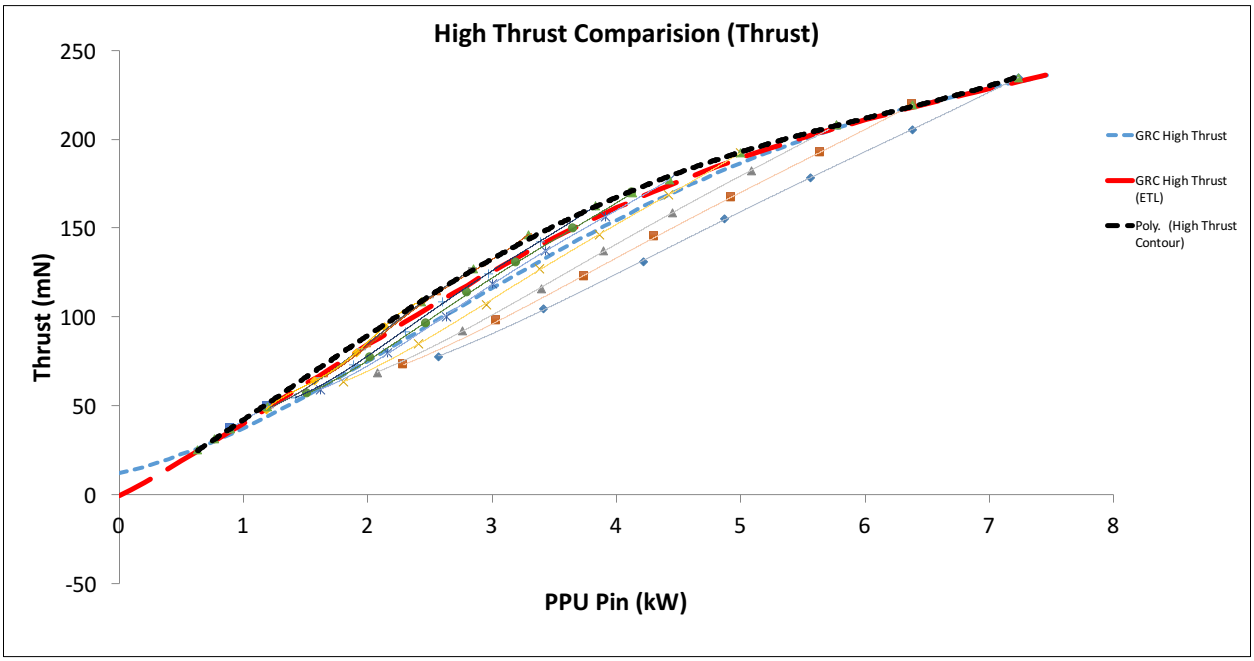

(a) High Thrust Comparison (Thrust)

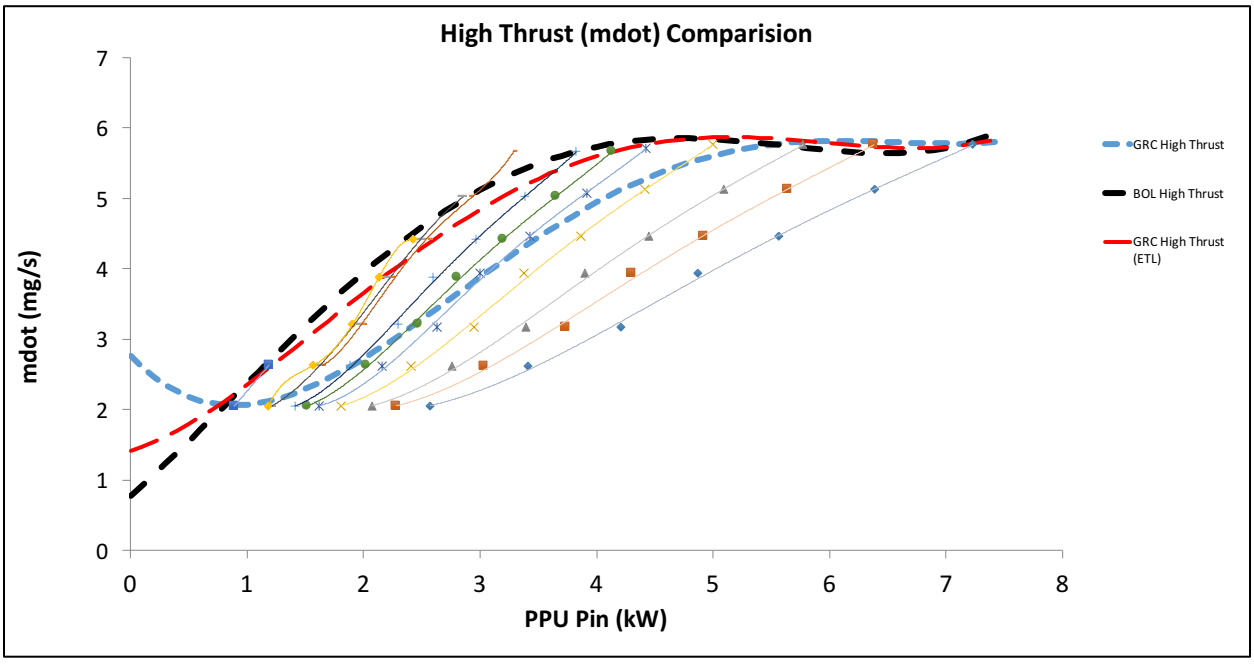

(b) High Thrust Comparison (m-dot)

Figure 6: Comparison of High Thrust Equations

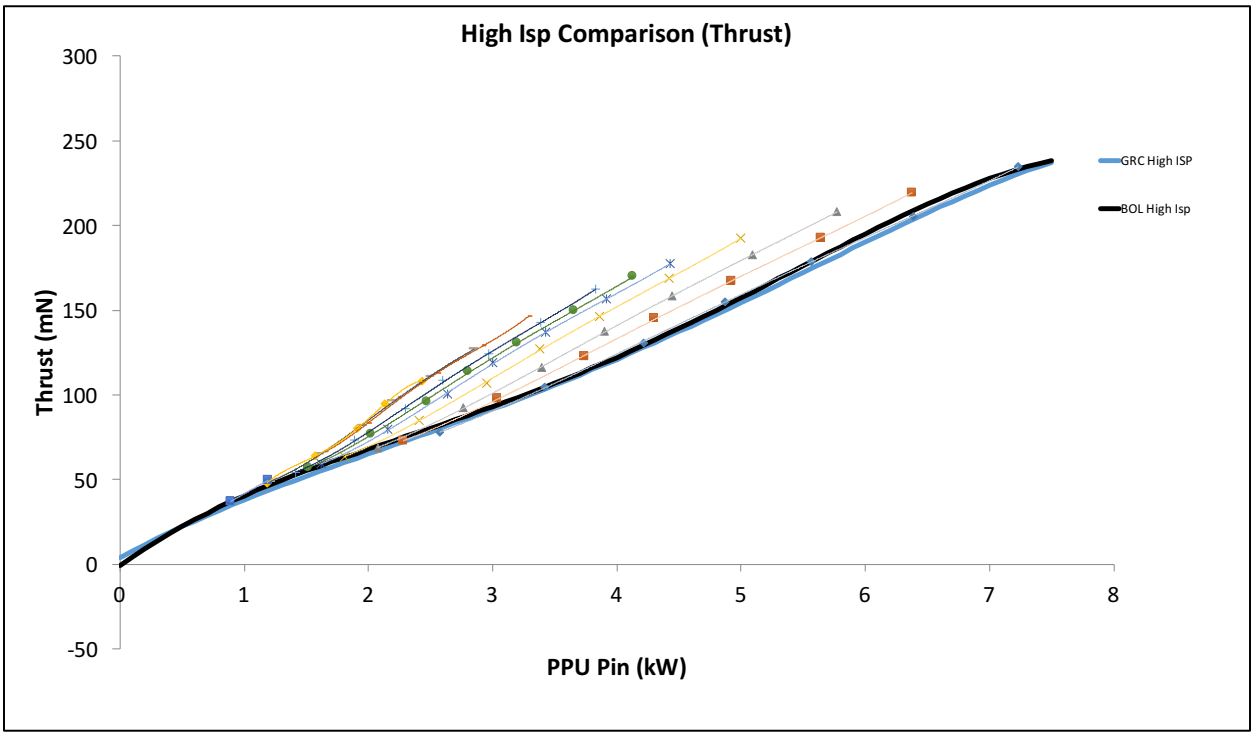

(a) High Isp Comparison (Thrust)

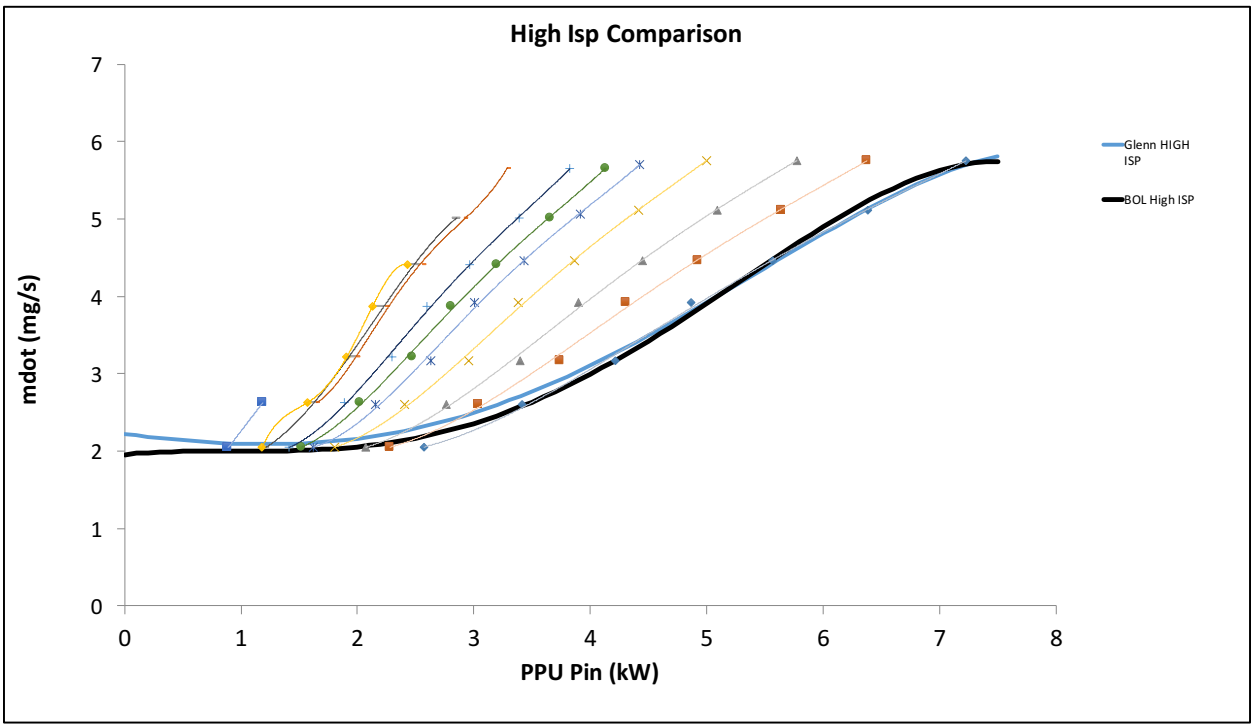

(b) High Isp Comparison (m-dot)

Figure 7: Comparison of High Isp Equations

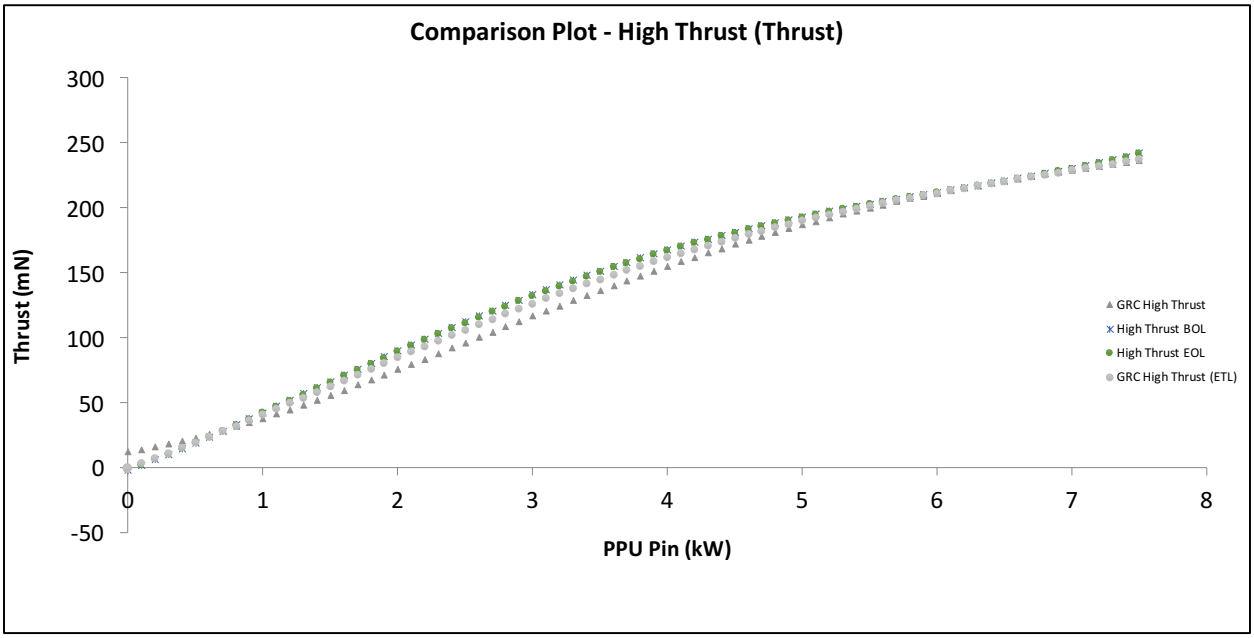

(a) High Thrust (thrust)

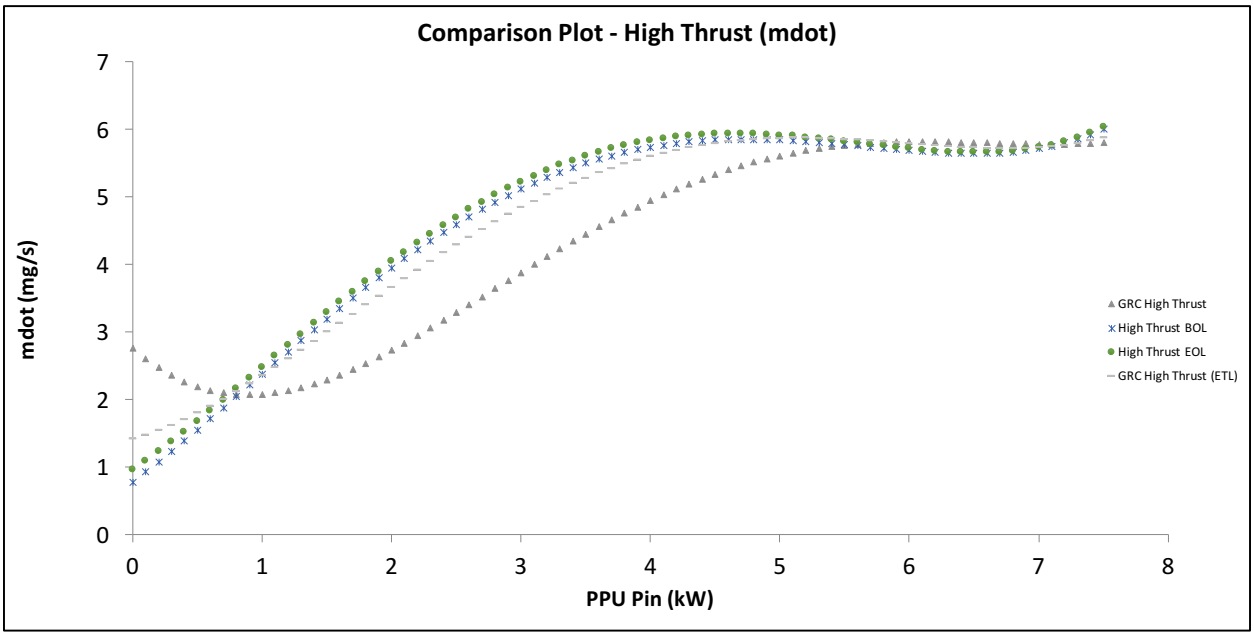

(b) High Thrust (mdot)

Figure 8: Comparison plots for High Thrust

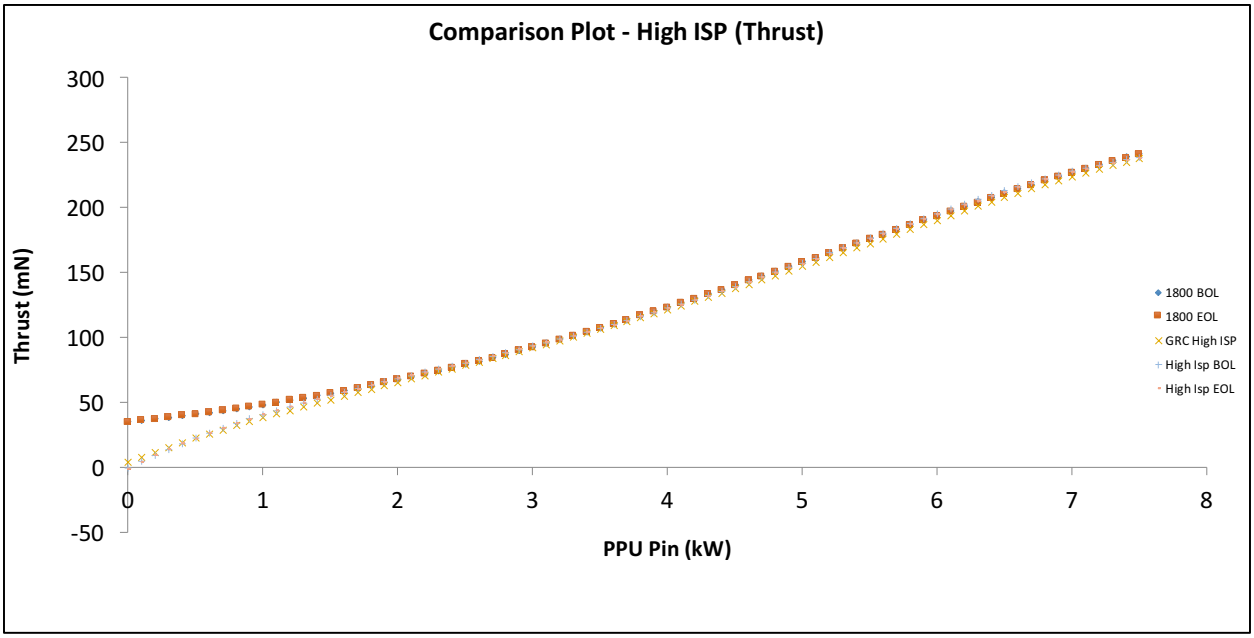

(a) High Isp (thrust)

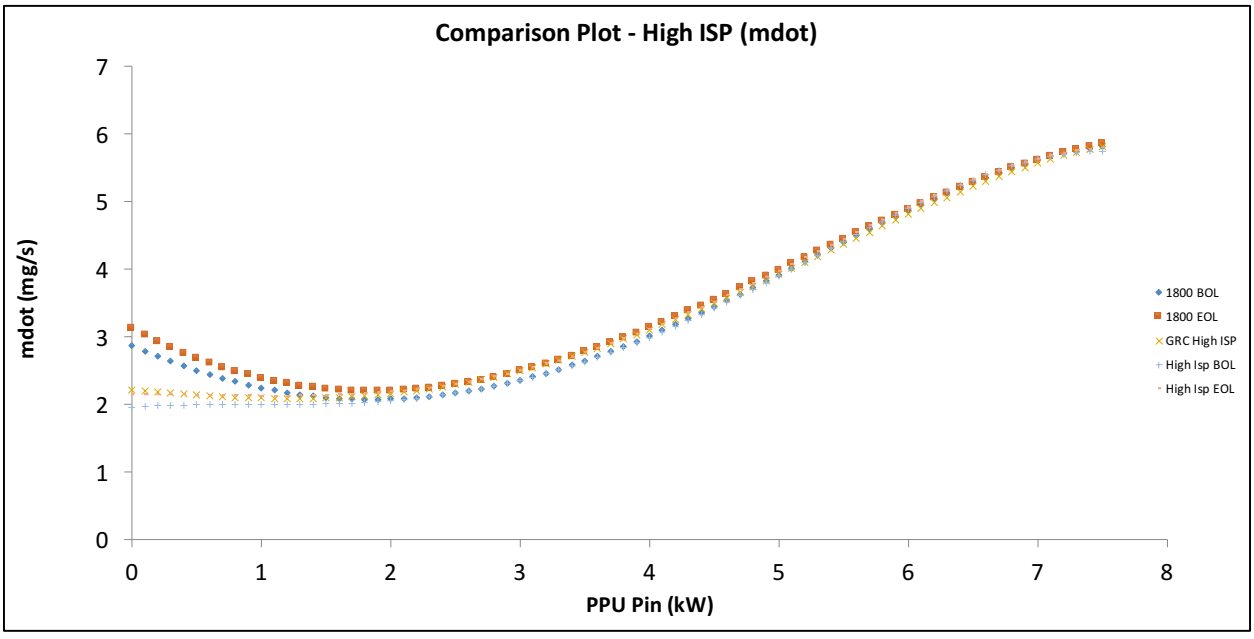

(b) High Isp (mdot)

Figure 9: Comparison plots for High Isp

III. Mission Analysis

EMTG[5] is an in-house NASA GSFC flight dynamics low thrust global optimizer that provides solutions for various mission criteria. Starting with user-inputs of thrust and mass flow rate curves, along with other constraints, EMTG produces a full mission solution. Therefore, by creating a custom mission using data-based thrust and mass flow rate curves, one can produce a better visual on the effects of the different curves on the thruster and mission.[6–8]

EMTG has previously been used in support of the OSIRIS-Rex Step 2 New Frontiers proposal and subsequently for Phase C work on that mission. In addition, EMTG is being used to support the Asteroid Redirect Robotic Mission (ARRM).[9] EMTGs low-thrust design capability is based on the medium-fidelity Sims-Flanagan transcription and launch vehicle, and power system models[5] which are industry standard for this type of design. EMTGs modeling is therefore nearly identical to that employed in other industry-standard tools such as MALTO,[10] GALLOP,[11] PAGMO,[12] and COLTT.[13] Like other industry-standard tools, EMTG uses SPICE for all planetary and small-body ephemerides.[14]

A. Validation

The following paragraphs describe two classic test problems (DAWN and NEARER) from the literature[15] which are relevant to small-body mission design. EMTG and MALTO, NASA Jet Propulsion Laboratory's (JPL) equivalent tool, are used to provide missions solutions to these problems. These solutions are checked for consitency to help determine ensure EMTG's validation.

Tables 4 and 5 below describe these mission parameters and contain the constraints set in EMTG for each respective mission. NEARER has more requirements as it a much more complicated mission. Linear models (NEXT thruster curves) have been used for thrusters in each of these runs in the literature. These benchmark problems were originally created in order to certify the HILTOP14[15] tool for pre-phase A mission design and so are appropriate for the same task for EMTG.

Array power at 1 AU	10.3 kW
Array performance model	$1/r^2$
Duty cycle	100%
Spacecraft bus power	0.25 kW
Thruster	1 NEXT
Launch vehicle	Delta II 2925-9.5
	no contingency
Launch declination limits	±28.5°
Thruster start delay (post-launch coast)	45 days
Launch date	9/27/2007
Mars flyby date	2/17/2009
Minimum periapse altitude at Mars	300 km
Vesta arrival	Any date in August 2011
Stay time at Vesta	270 days
Ceres arrival	Any date in February 2015

Table 4: Dawn mission parameters

Array power at 1 AU	6.5 kW
Array performance model	1/r^2
Duty cycle	100%
Housekeeping power	0.2 kW
Thruster	1 NEXT
Launch vehicle	Atlas V 401 NLS 1 contract performance 10% contingency
Launch declination limits	No constraints
Launch date	Anytime in 2014
Mission completion date	No later than 12/31/2021
Mass drop at Nereus	35 kg
Stay time at Nereus	60 days
Mass drop at Earth flyby	62 kg
Max v-infinity at flyby	6.7 km/s
Minimum Earth flyby altitude	300 km
Mass drop at 1996 FG3	30 kg
Stay time at 1996 FG3	60 days
Max v-infinity at return	6.7 km/s
Maximum propellant use	375 kg

Table 5: NEARER mission parameters

1. *DAWN*

The spacecraft (used in the mission optimizer) is identical to Dawn in all respects except that instead of using the NSTAR thruster, it uses an early version of the NEXT thruster. Also, because the two tools for which the problem was originally constructed, HILTOP and MALTO, had different propulsion modeling schemes, the NEXT performance model is linearized as follows:

$$T = a_t P + b_t$$

$$\dot{m} = a_f P + b_f$$

where T is thrust, $\dot{m}$ is mass flow rate, P is available power, and a_t is 7.282, $b_t = 32.901$, $a_f = 1.066$ and $b_f = 0.699$ are model coefficients.

The optimal solutions found using EMTG and MALTO are shown in Table 6. Note that the result found by the two tools are nearly identical, well within the bounds of acceptability for preliminary design. The only difference is that EMTG was able to improve the propellant use by 0.8 kg by moving the Mars flyby two weeks later than in the solution found using MALTO. This could be because of small (much less than 1 percent) modeling differences between the two medium-fidelity tools or because of a small bifurcation in the solution space where each tool went in a slightly different direction. The difference between the two solutions is negligible. A plot of the optimal trajectory found in EMTG is shown in Figure 10. Note: this solution is very similar to how all mission solutions are calculated throughout the paper.

Event	Location	Date		C3		Mass	
		EMTG	MALTO	EMTG	MALTO	EMTG	MALTO
Launch	Earth	9/27/2007	9/27/2007	5.1529	5.1529	1114.4	1114.4
Flyby	Mars	3/2/2009	2/18/2009	16.48	16.81	1040.2	1039.8
Arrival	Vesta	8/1/2011	8/1/2011			908.4	907.3
Departure	Vesta	4/27/2012	4/27/2012			908.4	907.3
Arrival	Ceres	2/28/2015	2/28/2015			808.0	807.2

Table 6: Comparison of the EMTG and MALTO solutions to the Dawn test problem

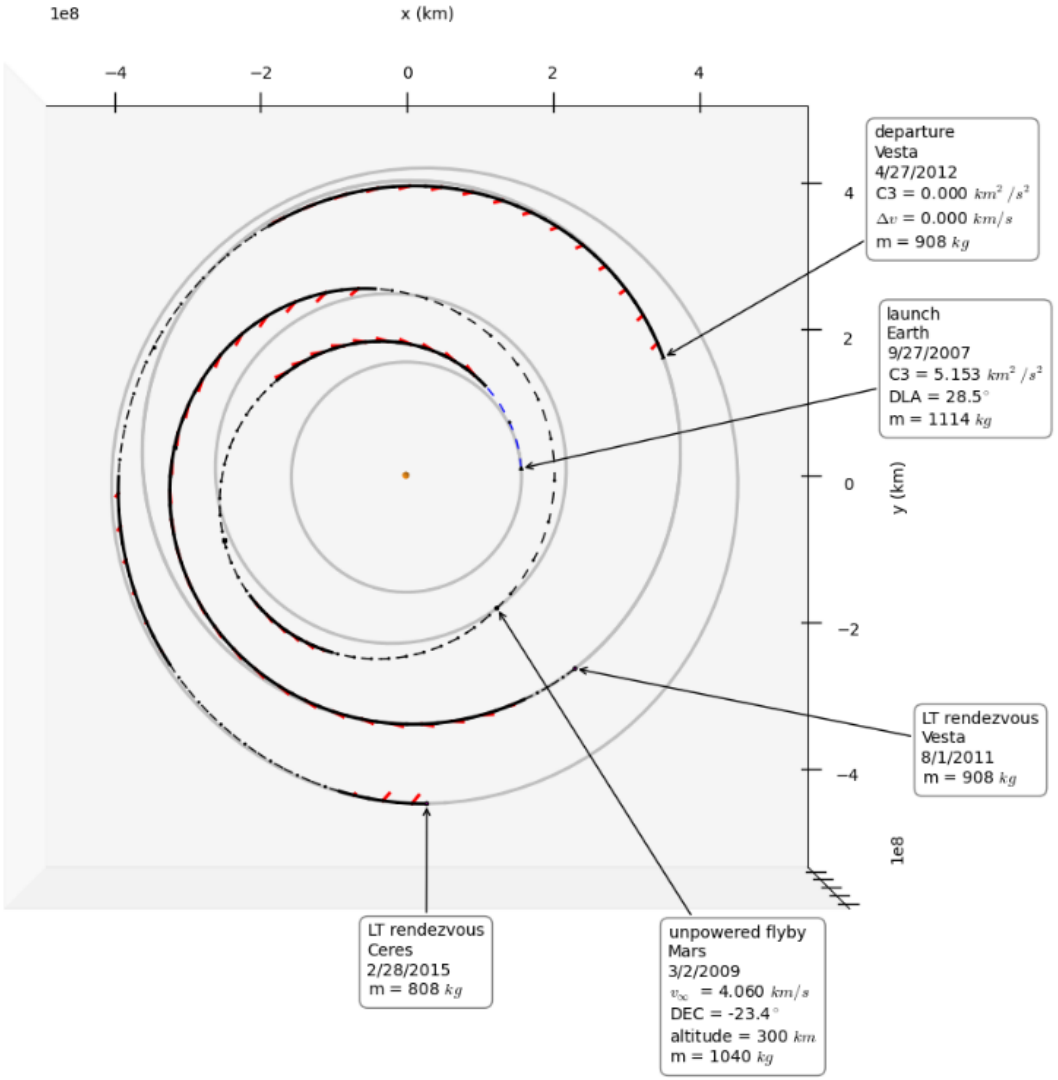

Figure 10: Optimal EMTG solution to the Dawn test problem

2. *NEARER*

The optimal solutions found by EMTG and MALTO are shown in Table 7. Two EMTG solutions are presented. The first solution forces EMTG to produce the same solution as MALTO. The solutions were very close: 808.7 kg final mass for EMTG vs 810.2 kg for MALTO, a difference of 0.2%.

This solution results in a violation of the propellant tank constraint by 1.5 kg. The small difference is due to the slight differences in modeling between the two tools and is not significant for preliminary design. After the first solution was found, EMTG was allowed to search the solution space more thoroughly and look for solutions that meet the constraints originally set but are not necessarily similar to the published MALTO trajectory. EMTGs global search mode identified a solution with a launch date in October 2014 instead of the published May 2014. This launch date enables a more efficient Earth to Nereus phase which allows a final mass of 830.5 kg. The optimal solution is shown in Figure 11.

Event	Location	Date			C3			Mass		
		EMTG #1	EMTG #2	MALTO	EMTG #1	EMTG #2	MALTO	EMTG #1	EMTG #2	MALTO
Launch	Earth	5/15/14	10/3/14	5/17/14	39.9	39.3	39.9	1312.2	1332.8	1312.2
Arrival	Nereus	6/22/16	6/20/16	6/24/16				1125.4	1150.4	1129.3
Departure	Nereus	8/21/16	8/19/16	8/23/16				1090.4	1115.4	1094.3
Flyby	Earth	2/1/18	2/3/18	2/4/18	39.2	39.6	44.5	960.2	986.4	963.7
Arrival	1996 FG3	5/14/20	5/6/20	6/4/20				891.7	915.5	893.0
Departure	1996 FG3	8/1/20	7/27/20	8/3/20				861.7	885.5	863.0
Arrival	Earth	6/21/21	6/21/21	6/21/21	44.9	44.9	44.9	808.7	830.8	810.2

Table 7: Comparison of the EMTG and MALTO solutions to the NEARER test problem

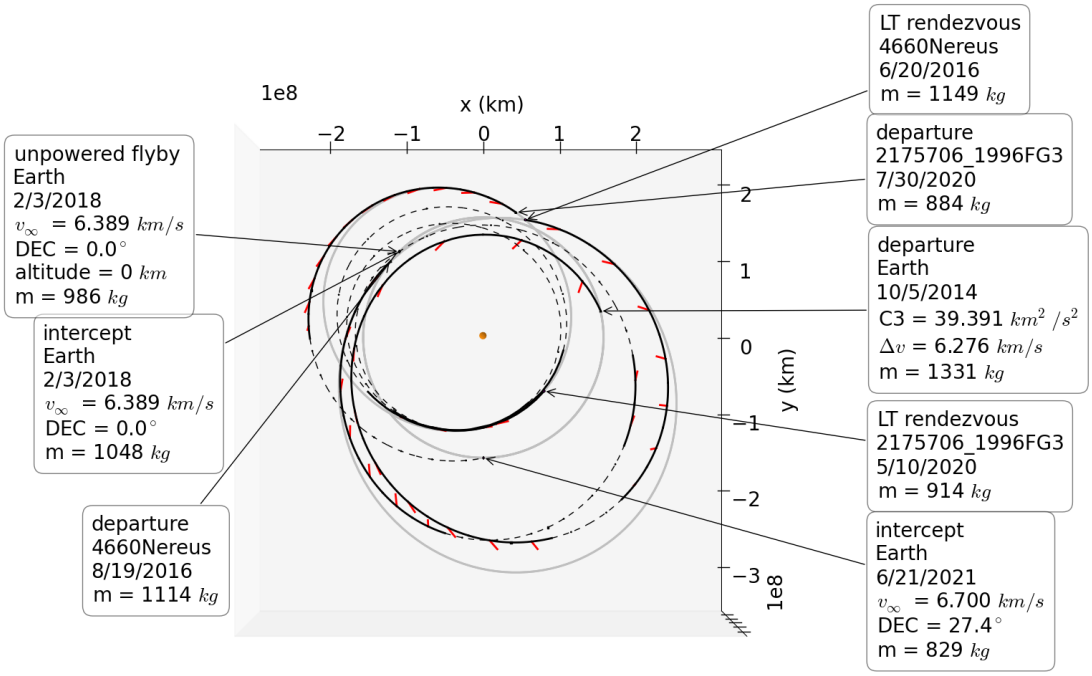

Figure 11: Optimal solution to the NEARER test problem

The examples presented above demonstrate that EMTGs modeling fidelity is sufficient for preliminary design and is equivalent, if not superior, to the commonly used MALTO tool. The differences between

EMTGs modeling and that of other medium-fidelity tools are significantly less than the difference between any medium-fidelity design and the eventual high-fidelity design.

B. EMTG Customization

Customization for EMTG is broken up into three categories: global mission options, spacecraft options and journey options. The global mission parameter options include mission launch dates, duration bounds and locations of launch. Spacecraft options primarily deal with power and propulsion of the mission. The launch vehicle as well as the thruster can be changed. Custom thruster curves can also be input to the system. Power sources for the spacecraft can either be solar or radioisotope. A power model and a decay rate can also be implemented.

In this work, an Earth to Mars mission was designed as a control to test each of the throttle curves in EMTG. It was a 3 year mission with a 30 day launch date window. A successful mission scenario occurs when the spacecraft launches from Earth, reaches rendezvous with Mars and performs a "spiral down" landing procedure. All parameters are set constant when changing between different throttle curves. Table 8 contains this information. Three optimization variables were chosen for EMTG. They were maximizing payload mass, minimizing time (final mass constraint set), and minimizing BOL power (reducing the size of the solar array).

Array power at 1 AU	10 kW
Array performance model	$1/r^2$
Duty cycle	90%
Thruster	1 NEXT
Launch vehicle	Atlas V
Launch declination limits	-28.5°
Launch date	1/16/2016

Table 8: EMTG contraints: Earth to Mars

C. Results

In the following tables, the modified 1800 V curves from both the BOL and EOL along with their respective high thrust curves are being compared to the NASA GRC high thrust (baseline and ETL) and Isp curves. Figure 12 compares the high Isp curves with the 1800 V BOL and EOL modified curves. Figure Figures 13 compares the high thrust curves. Tables 19, 20, and 21 (Appendix A) present the data collected from EMTG for each optimization.

Figures 12a, 12b, and 12c present results from the high ISP curves and 1800 V curves. Figure 12a displays how much propellant was used during each mission. For solutions optimized for maximizing final mass, the 1800 V BOL curves used the least amount of propellant where as the EOL high ISP curve and GRC high ISP curves used the most amount of propellant. The solutions vary by a few kg's of propellant, which is still significant for such a small mission. When optimizing for minimum time, all missions used the same amount of propellant due to a final mass constraint (mentioned above). The maximum propellant allowable for this mission was 125 kg (525 kg (initial mass) - 400 kg (maximum final mass)). This helps further solidify EMTG's ability to implement mission constraints into its optimization scheme. Lastly, when looking at minimizing BOL power, the BOL/EOL high Isp curves used the most amount of propellant.

Figure 12b shows the total trip time for all optimization (for high Isp curves). For all three optimizations, the total trip time only varies by tens of days between each curve. Figure 12c shows the peak power generated (right after launch) for each of the three optimizations. Once again, there isn't a large difference between each of the curves for peak power generated. The GRC high Isp curve does necessitate a slightly larger solar array when minimizing for BOL power.

The high thrust curves shown in Figures 13a, 13b and 13c show that the GRC high thrust curve used the least amount of propellant when maximizing final mass to produce similar trip times which is counter-intuitive since a high thrust curve should use more propellant to achieve shorter trip times. This is addressed in the discussion section below. The GRC ETL curve used about the same amount of propellant as the BOL/EOL high thrust curves. All of the high thrust curves used the same amount of propellant when optimizing for

minimum time and minimum BOL power. The high thrust curves also had very similar trip times for each optimization.

When looking at peak power generated (Figure 13c), there is variation when the curves were optimizing towards minimum BOL power. The GRC curves have a higher peak power than the other curves, failing to minimize BOL power.

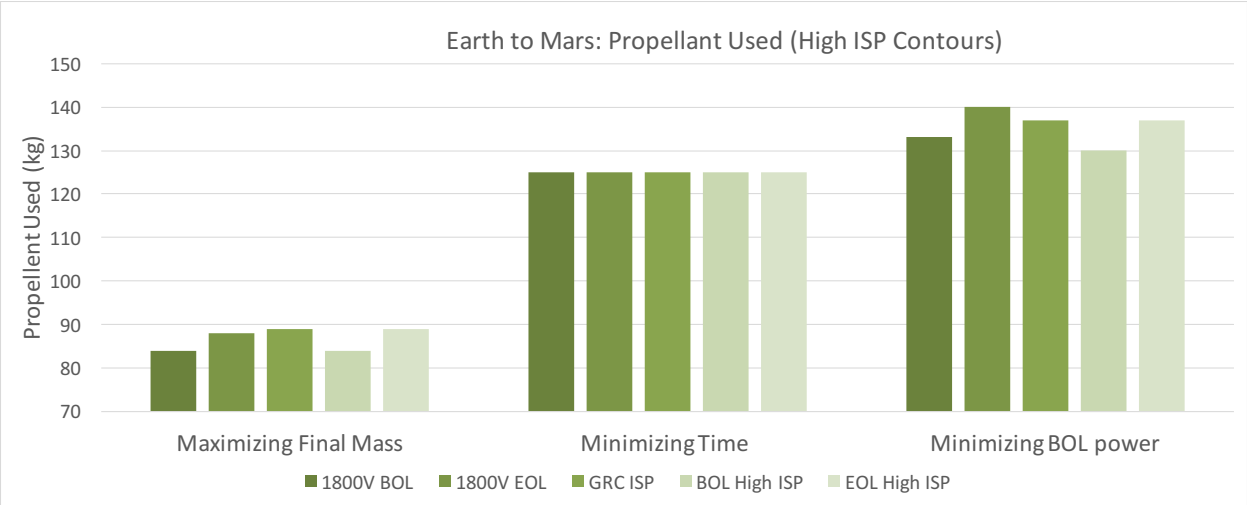

(a) High ISP curves - comparing propellant used

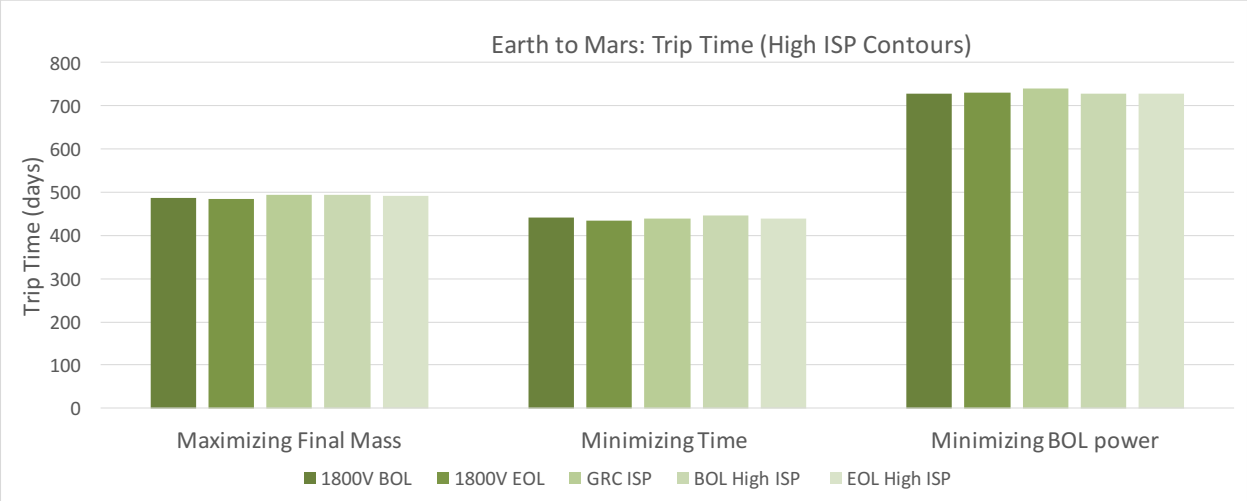

(b) High ISP curves - comparing total trip time

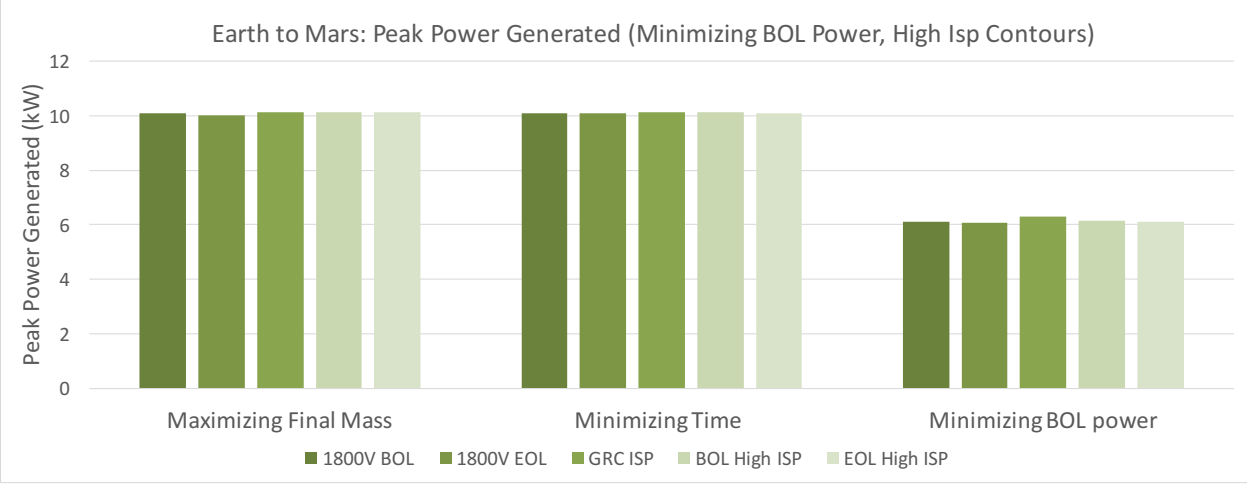

(c) High ISP curves - comparing peak power used

Figure 12: Earth to Mars results: High Isp

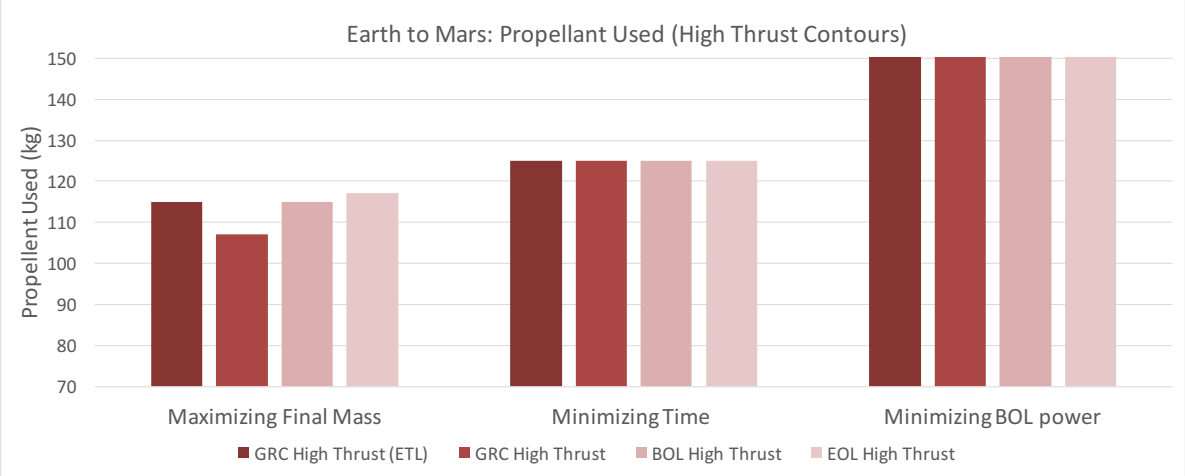

(a) High thrust curves - comparing propellant used

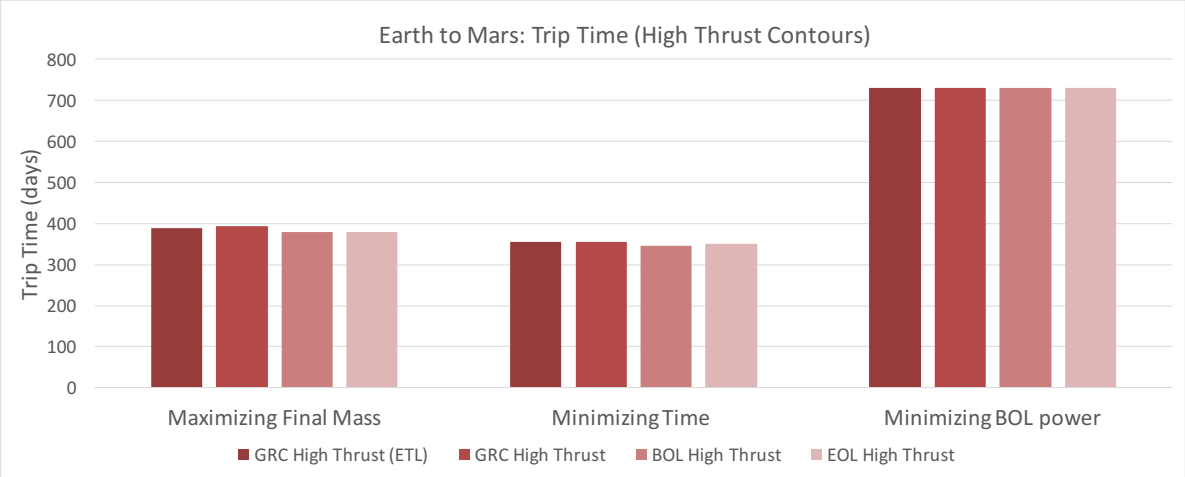

(b) High thrust curves - comparing total trip time

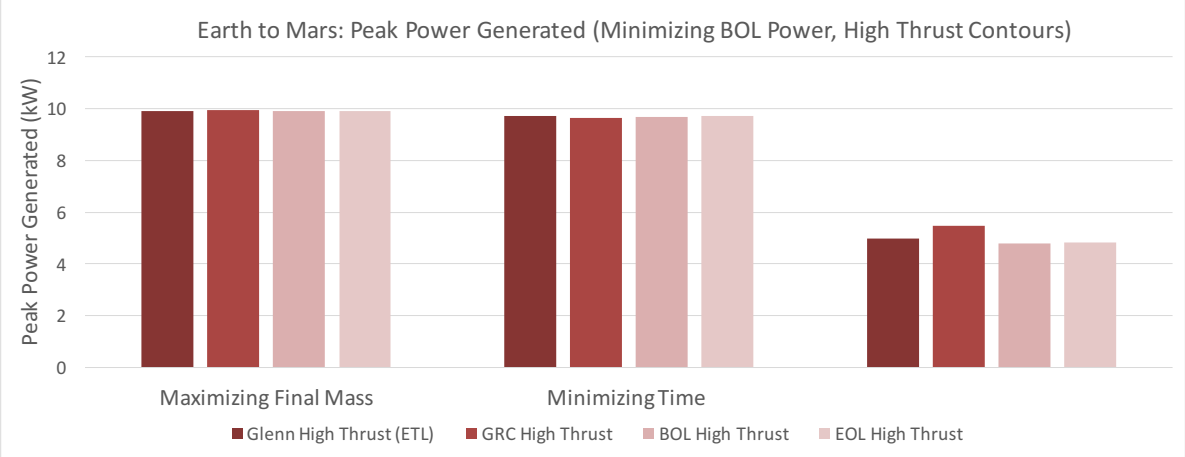

(c) High thrust curves - comparing comparing peak power used

Figure 13: Earth to Mars results: High Thrust

IV. Discussion

There are two specific findings of note within the high thrust solutions. The first is propellant usage when optimizing for maximum final mass (Figure 13a). The GRC high thrust curve produced similar trip times as the other curves when maximizing final mass but required much less propellant. This is because the GRC high thrust curve uses only the regular throttle points instead of the extended throttle table, allowing EMTG to access the lower power levels of NEXT. Therefore, the GRC high thrust curve has a higher Isp than the GRC ETL curve, resulting in a solution that didn't require as much propellant.

The second discrepancy within the high thrust curve solutions occurs when optimizing for BOL power (Figure 13c). The GRC high thrust curve requires almost 0.8 kW more power (when compared to other high thrust curves) in a case that minimizes BOL power. The GRC high thrust ETL curve and the BOL/EOL high thrust curves developed here provide the best results for a power-constrained mission.

The GRC high Isp curves performed relatively well when compared to the high Isp curves created here. Most of the solutions required similar amounts of propellant and total trip time. When optimizing for maximum final mass, the GRC high Isp curve falls between the BOL and EOL curve for high Isp. Similarly, it fell in between the 1800 V BOL and EOL curve for propellant usage when minimizing BOL power.

The reason why the high thrust curves differ more than the high Isp curves is due to the throttle points the GRC curves seem to be generated from. The GRC high Isp curve (Figure **??**) use almost the same throttle points as BOL/EOL high Isp curves (Figure **??**) except at low beam current levels (at 1800 beam power supply voltage). Such a small difference resulted in only small variations between mission solutions. The high thrust curves, on the other hand, have more noticeable variations between mission solutions. This is due to the GRC high thrust and GRC high thrust ETL curves using throttle points (Figure **??**) that don't fully maximized towards high thrust (when compared to the BOL/EOL high thrust curves shown in Figure **??**).

In general, the new curves generated here for thrust produce lower trip time solutions and the high Isp curves produce lower propellant required solutions when compared to the GRC high thrust and high Isp curves. In each of the tests, results have differed on the order of days for trip time and kg's for propellant. Specific to the Earth to Mars mission, on average, propellant variation is around 10 kg between two extremes. When optimizing for maximizing final mass, as shown in Figures 12a and 13c, this would be more than a 10 percent change in propellant use. Although the percent change on the overall trip time between curves isn't as high with only a few days variation against an overall trip time that is a few hundreds of days (Figures 12b and 13b), it does represent mission solution variations that need to be accounted for.

In addition to differences between BOL/EOL and GRC curves, it is shown that BOL and EOL do not produce the same results in any scenario, indicating the effect of thruster degradation, as mentioned previously. Improvements to this would require an interpolation method in order to properly address any performance decrease of the thruster, which currently does not exist. Nevertheless, a single curve is not sufficient to describe thruster performance as demonstrated by the difference in mission solutions among the BOL, EOL and GRC curves.

V. Conclusion

From the work done in this paper, it is seen that existing curves for NEXT are not sufficient to characterize its performance. Optimal performance of a given mission was characterized by propellant mass, total trip time and peak-power (size of solar array). The GRC high thrust and high Isp curves do not fully maximize thrust and Isp respectively. Small variations between the GRC curves and the ones generated in this paper result in different solutions to an optimized mission-design. For high thrust, curves that follow the ETL perform better for power-constrained missions and the non-ETL high thrust curves perform better for propellant constrained missions. Furthermore, thruster degradation needs to be accounted for as well.

Acknowledgments

The authors would like to thank the Harriett Jenkins Graduate Fellowship for funding this research as well as Mike Patterson for consulting on the throttle table.

References

[1]Garner, R., "NASA's Goddard, Glenn Centers Look to Lift Space Astronomy out of the Fog," March 2012, [Online; posted 03-March-2012].

[2]Soulas, C. G. and Patterson, M. J., "NEXT Ion Thruster Performance Dispersion Analyses," .

[3]Herman, D. A., Soulas, G. C., Van Noord, J. L., and Patterson, M. J., "NASAs Evolutionary Xenon Thruster Long-Duration Test Results," *Journal of Propulsion and Power*, Vol. 28, No. 3.

[4]"NEXT Document for Discovery 2014 AO Library," .

[5]Englander, J. A., Ellison, D. H., and Conway, B. A., "Global Optimization of Low-Thrust, Multiple-Flyby Trajectories at Medium and Medium-High Fidelity," .

[6]Englander, J. A., Vavrina, M. A., Naasz, B., Merill, R. G., and Qu, M., "Mars, Phobos, and Deimos Sample Return Enabled by ARRM Alternative Trade Study Spacecraft," .

[7]Englander, J., *Automated Trajectory Planning For Multiple-Flyby Interplanetary Missions*, Ph.D. thesis, University of Illinois at Urbana-Champaign, Illinois, 2013.

[8]Englander, J. A. and Englander, A. C., "Tuning Monotonic Basin Hopping: Improving the Efficiency of Stochastic Search as Applied to Low-Thrust Trajectory Optimization," .

[9]Englander, J., Vavrina, M., Naasz, B., Merill, R., and Qu, M., "Mars, Phoos, and Deimos Sample Return Enabled by ARRM Alternative Trade Study Spacecraft," .

[10]Sims, J. A., Finlayson, P., Rinderle, E., Vavrina, M., and Kowalkowski, T., "Implementation of a low-thrust trajectory optimization algorithm for preliminary design," .

[11]McConaghy, T., Debban, T., Petropolous, A., and Longuski, J., "Design and Optimization of Low-Thrust Trajectories with Gravity Assists," *Journal of Spacecraft and Rockets*, Vol. 40.

[12]Yam, C., Di Lorenzo, D., and Izzo, D., "Low-Thrust Trajectory Design as a Constrained Global Optimization Problem," *Part G: Journal of Aerospace Engineering*, Vol. 225.

[13]Herman, J., Zimmer, A., Reijneveld, J., Dunlop, K., Takahashi, Y., Tardivel, S., and Scheeres, D., "Human Exploration of Near Earth Asteroids: Mission Analysis for a Chemical and Electric Propulsion Mission," *Acta Astronautica*.

[14]"Spice Ephemeris," DOI: 10.1016/j.actaastro.2014.07.034.

[15]Horsewood, Jerry, L. and Dankanich, J. W., "Heliocentric Interplanetary Low-thrust Trajectory Optimization Program Capabilities and Comparison to NASAs Low-thrust Trajectory Tools," .

Appendix

The following tables show all the fit lines generated along with GRC curves. In all instances, x represents P_{in} (input power).

Table 9: Thrust fit-line equations at BOL

V_{bsp}	Thrust Equation (mN)
High ISP	$T(x) = -0.200394396x^4 + 3.09602667x^3 - 14.79371475x^2 + 53.24364773x - 0.880568326$
High Thrust	$T(x) = 0.1384351^4 - 2.057211x^3 + 6.6882331x^2 + 39.7097107132x - 2.38859651$
1800	$T(x) = -0.041430321x^4 + 0.2968243x^3 + 2.37060001x^2 + 10.5258144x + 34.992831$
1567	$T(x) = 0.2593x^4 - 4.8436x^3 + 32.794x^2 - 58.542x86.249$
1396	$T(x) = 0.3078x^4 - 5.5039x^3 + 35.458x^2 - 58.533x81.189$
1179	$T(x) = 0.8335x^4 - 12.225x^3 + 65.03x^2 - 106.65x107.18$
1021	$T(x) = 1.7125x^4 - 22.389x^3 + 105.28x^2 - 166.54x + 136.17$
936	$T(x) = 1.7449x^4 - 21.46x^3 + 95.07x^2 - 134.58x + 108.06$
850	$T(x) = 2.8792^4 - 32.368x^3 + 131.64x^2 - 182.47x + 129.3$
700	$T(x) = 15.072x^4 - 149.14x^3 + 539.43x^2 - 794.55x + 467.02$
679	$T(x) = 3.3676x^4 - 37.335x^3 + 143.66x^2 - 180.2x + 115.69$
650	$T(x) = -76.018x^4 + 536.65x^3 + -1380.4x^2 + 1579.2x - 627.97$
400-275	$T(x) = -54.185x^3 + 141.54x^2 - 75.69x + 30.498$

Table 10: Mass flow rate fit-line equations at BOL

V_{bsp}	Mass Flow Rate (mg/s)
High ISP	$m(x) = -0.005987542x^4 + 0.074628525x^3 - 0.175668526x^2 + 0.151098815x + 1.956250894$
High Thrust	$m(x) = 0.0084761x^4 - 0.1113601x^3 + 0.2587433x^2 + 1.44382383x + 0.7717598$
1800	$m(x) = -0.00266205x^4 + 0.0150629x^3 + 0.20069186x^2 - 0.83824381x + 2.8759130$
1567	$m(x) = 0.0118x^4 - 0.2377x^3 + 1.712x^2 - 4.2632x + 5.3694$
1396	$m(x) = 0.0161x^4 - 0.3012x^3 + 2.0117x^2 - 4.5961x + 5.3217$
1179	$m(x) = 0.0355x^4 - 0.5574x^3 + 3.1474x^2 - 6.2963x + 6.0651$
1021	$m(x) = 0.0812x^4 - 1.0969x^3 + 5.3349x^2 - 9.6331x + 7.762$
936	$m(x) = 0.0873x^4 - 1.0939x^3 + 4.9409x^2 - 8.0383x + 6.2311$
850	$m(x) = 0.1266x^4 - 1.4707x^3 + 6.1652x^2 - 9.42x + 6.6949$
700	$m(x) = 1.0409x^4 - 10.375x^3 + 37.864x^2 - 57.984x + 34.106$
679	$m(x) = 0.0535x^4 - 0.0992x^3 + 2.0944x^2 - 3.3188x + 3.2846$
650	$m(x) = -5.6594x^4 + 40.367x^3 - 105.1x^2 + 120.06x - 48.65$
400-275	$m(x) = -17.475x^3 - 45.14x^2 + 38.754x^2 - 9.0094$

Table 11: Thrust fit-line equations at EOL

V_{bsp}	Thrust Equation (mN)
High ISP	$T(x) = -0.196896539x^4 + 3.05918604x^3 - 14.72524921x^2 + 53.32445536x - 1.335725134$
High Thrust	$T(x) = 0.13701397x^4 - 2.05900345x^36.8929834x^2 + 38.74487882x + 2.250668$
1800	$T(x) = -0.0405432x^4 + 0.29083768x^3 + 2.3320396x^2 + 10.6571918x + 34.687332$
1567	$T(x) = 0.2534x^4 - 4.7545x^3 + 32.34x^2 - 57.84x + 85.831$
1396	$T(x) = 0.2996x^4 - 5.3855x^3 + 34.883x^2 - 57.68x + 80.699$
1179	$T(x) = 0.809x^4 - 11.937x^3 + 63.874x^2 - 105.15x + 106.51$
1021	$T(x) = 1.6564x^4 - 21.802x^3 + 103.2x^2 - 164.07x + 135.23$
936	$T(x) = 1.6806x^4 - 20.82x^3 + 92.899x^2 - 132.08x + 107.07$
850	$T(x) = 2.7668x^4 - 31.346x^3 + 128.46x^2 - 179.06x + 128.09$
700	$T(x) = 14.355x^4 - 143.34x^3 + 523.13x^2 - 776.89x + 460.99$
679	$T(x) = 3.2213x^4 - 36.011x^3 + 139.76x^2 - 176.44x + 114.53$
650	$T(x) = -71.839x^4 + 511.84x^3 - 1328.6x^2 + 1534.5x - 615.39$
400-275	$T(x) = -59.967x^3 + 158.93x^2 - 92.693x + 35.411$

Table 12: Mass flow rate fit-line equations at EOL

V_{bsp}	Mass Flow Rate (mg/s)
High ISP	$m(x) = -0.004792385x^4 + 0.057358188x^3 - 0.09987237x^2 + 0.032353523x + 2.137689593$
High Thrust	$m(x) = 0.0094585x^4 - 0.12660861x^3 + 0.3336997x^2 + 1.3059342x + 0.9485779$
1800	$m(x) = -0.001156113x^4 - 0.00786841x^3 + 0.31217985x^2 - 1.0476175x + 3.1343462$
1567	$m(x) = 0.0086x^4 - 0.1704x^3 + 1.2174x^2 - 2.7769x + 3.9603$
1396	$m(x) = 0.0113x^4 - 0.2107x^3 + 1.4067x^2 - 2.9458x + 3.9006$
1179	$m(x) = 0.0265x^4 - 0.4128x^3 + 2.3166x^2 - 4.3433x + 4.6092$
1021	$m(x) = 0.0479x^4 - 0.6627x^3 + 3.3035x^2 - 5.6585x + 5.1535$
936	$m(x) = 0.0682x^4 - 0.8811x^3 + 4.104x^2 - 6.6825x + 5.5781$
850	$m(x) = 0.0995x^4 - 1.1913x^3 + 5.1458x^2 - 7.8876x + 6.0038$
700	$m(x) = 0.967x^4 - 9.7669x^3 36.14x^2 - 56.095x + 33.612$
679	$m(x) = -0.0909x^4 + 0.2654x^3 + 0.8749x^2 - 1.6774x + 2.6339$
650	$m(x) = -5.6776x^4 + 40.975x^3 + -107.97x^2 + 124.74x - 51.056$
400-275	$m(x) = 16.961x^3 - 44.401x^2 + 38.632x - 8.9972$

Table 13: GRC high thrust thrust fit-line equations[4]

	Thrust (mN)
GRC thrust	$T(x) = 0.101855017x^4 - 2.04053417x^3$ $+ 11.4181412x^2 + 16.0989424x + 11.9388817$

Table 14: GRC high thrust mass flow rate fit-line equations[4]

	Mass Flow Rate (mg/s)
GRC mdot	$m(x) = 0.011021367x^4 - 0.207253445x^3$ $+ 1.216702370x^2 - 1.71102132x + 2.75956482$

Table 15: GRC high thrust (ETL) thrust fit-line equations[4]

	Thrust (mN)
GRC ETL thrust	$T(x) = 0.085120672x^4 - 1.42659172x^3$ $+ 5.17797704x^2 + 37.1873936x + -0.804281458$

Table 16: GRC high thrust (ETL) mass flow rate fit-line equations[4]

	Mass Flow Rate (mg/s)
GRC mdot	$m(x) = 0.009019519x^4 - 0.138009326x^3$
	$+ \quad 0.535910391x^2 0.534442545x + 1.40535083$

Table 17: GRC high Isp thrust fit-line equations[4]

	Thrust (mN)
GRC thurst	$T(x) = -0.111563126x^4 + 1.72548416x^3$
	$+ \quad -7.91621814x^2 + 40.543251x + 3.68945763$

Table 18: GRC high Isp mass flow rate fit-line equations[4]

	Mass Flow Rate (mg/s)
GRC mdot	$T(x) = -0.00291399146x^4 + 0.0298873982000000x^3$
	$+ \quad 0.0277715756x^2 - 0.180919262x + 2.22052155$

Table 19: Earth to Mars - Optimizing Mass

Thrust Curves	Launch Date	Rendezvous Date	End Spiral	Total Trip Time (days)	Initial Mass (kg)	Final Mass (after spiral) (kg)	Propellant Used (kg)	Peak Power Generated (kW)
1800 BOL	02/26/16	01/20/17	06/27/17	487	525	441	84	10.1
1800 EOL	02/26/16	01/18/17	06/24/17	484	525	437	88	10
BOL High Thrust	03/08/16	12/11/16	03/22/17	379	525	410	115	9.9
EOL High Thrust	03/08/16	12/11/16	03/22/17	379	525	408	117	9.9
BOL High ISP	02/12/16	01/14/17	06/19/17	493	525	441	84	10.11
EOL High ISP	02/12/16	01/13/17	06/18/17	492	525	437	88	10.12
Glenn High Thrust	03/04/16	12/19/16	04/12/17	404	525	418	107	9.93
Glenn High Thrust (ETL)	03/06/16	12/14/16	03/29/17	388	525	409	116	9.91
Glenn ISP	02/12/16	01/14/17	06/19/17	493	525	436	89	10.11

Table 20: Earth to Mars - Optimizing Time

Thrust Curves	Launch Date	Rendezvous Date	End Spiral	Total Trip Time (days)	Initial Mass (kg)	Final Mass (after spiral) (kg)	Propellant Used (kg)	Peak Power Generated (kW)
1800_BOL	02/07/16	12/11/16	04/24/17	442	525	400	125	10.1
1800_EOL	02/16/16	12/12/16	04/26/17	435	525	400	125	10.09
BOL High Thrust	03/27/16	11/30/16	03/07/17	345	525	400	125	9.69
EOL High Thrust	03/24/16	12/01/16	03/09/17	350	525	400	125	9.72
BOL High ISP	02/08/16	12/13/16	04/28/17	445	525	400	125	10.13
EOL High ISP	02/12/16	12/13/16	04/28/17	441	525	400	125	10.08
Glenn High Thrust	03/29/16	12/02/16	03/19/17	355	525	400	125	9.64
Glenn High Thrust (ETL)	03/24/16	12/03/16	03/14/17	355	525	400	125	9.71
Glenn ISP	02/12/16	12/10/16	04/26/17	439	525	400	125	10.14

Table 21: Earth to Mars - Optimizing Power

Thrust Curves	Launch Date	Rendezvous Date	End Spiral	Total Trip Time (days)	Initial Mass (kg)	Final Mass (after spiral) (kg)	Propellant Used (kg)	Peak Power Generated (kW)
1800_BOL	01/16/16	04/20/17	01/14/18	729	525	392	133	6.11
1800_EOL	01/16/16	04/21/17	01/15/18	730	525	385	140	6.09
BOL High Thrust	01/16/16	03/26/17	01/14/18	729	525	337	188	4.79
EOL High Thrust	01/16/16	03/27/17	01/14/18	729	525	330	195	4.82
BOL High ISP	01/16/16	04/12/17	01/14/18	729	525	396	129	6.14
EOL High ISP	01/16/16	04/13/17	01/14/18	729	525	388	137	6.12
Glenn High Thrust	01/16/16	03/27/17	01/14/18	729	525	366	159	5.49
Glenn High Thrust (ETL)	01/16/16	03/28/17	01/14/18	729	525	339	186	4.99
Glenn ISP	01/16/16	04/10/17	01/14/18	729	525	388	137	6.31